Distribution Agreement

In presenting this thesis or dissertation as a partial fulfillment of the requirements for an advanced degree from Emory University, I hereby grant to Emory University and its agents the non-exclusive license to archive, make accessible, and display my thesis or dissertation in whole or in part in all forms of media, now or hereafter known, including display on the world wide web. I understand that I may select some access restrictions as part of the online submission of this thesis or dissertation. I retain all ownership rights to the copyright of the thesis or dissertation. I also retain the right to use in future works (such as articles or books) all or part of this thesis or dissertation.

Signature:

_____ _____

Teresa Emerick Madsen Date

Corticolimbic Oscillations in Fear Learning

By

Teresa Emerick Madsen
Doctor of Philosophy

Graduate Division of Biological and Biomedical Science
Neuroscience

_____
Donald G. Rainnie, Ph.D.
Advisor

_____
Elizabeth Buffalo, Ph.D.
Committee Member

_____
Joseph Manns, Ph.D.
Committee Member

_____
Helen Mayberg, M.D.
Committee Member

_____
Kerry Ressler, M.D., Ph.D.
Committee Member

Accepted:

_____
Lisa A. Tedesco, Ph.D.
Dean of the James T. Laney School of Graduate Studies

_____
Date

Corticolimbic Oscillations in Fear Learning

By

Teresa Emerick Madsen
B.A., Grinnell College, 2004

Advisor: Donald G Rainnie, Ph.D.

An abstract of
A dissertation submitted to the Faculty of the
James T. Laney School of Graduate Studies of Emory University
in partial fulfillment of the requirements for the degree of
Doctor of Philosophy
in
Graduation Division of Biological and Biomedical Science
Neuroscience
2014

Abstract

Corticolimbic Oscillations in Fear Learning
By Teresa Emerick Madsen

Neural oscillations are thought to mediate efficient communication of related information across distant brain regions and contribute to the long term synaptic alterations that underlie memory. Recently, many neuropsychiatric disorders have been correlated with unique "spectral fingerprints," *i.e.*, patterns of disruption in EEG or MEG recordings of neural oscillations. However, little is known about the role of these oscillations in normal emotion.

The functional anatomy of the corticolimbic system – the collection of brain regions most implicated in emotion and neuropsychiatric disorders – has been thoroughly studied within the context of Pavlovian fear conditioning in rodents. Here, the basolateral complex of the amygdala (BLA) and medial prefrontal cortex (mPFC) have been identified as critical nodes with distinct roles in the acquisition and extinction of fear memory.

Using multielectrode recording of LFPs in the mPFC and BLA of freely moving rats, we investigated functional interactions between these two regions during fear conditioning and extinction. Both regions displayed significantly increased power, and coherence between regions, in a sharply tuned delta/theta (2-6 Hz) band during successful fear acquisition and recall, as compared to baseline (before habituation tones). Throughout fear acquisition, the mid-gamma (45-60 Hz) range was significantly elevated over baseline in terms of mPFC power, BLA power, and coherence between the two regions. After the shock, there were dramatic increases in high gamma (60-90 Hz) power for the mPFC and in low gamma (30-45 Hz) power for the BLA, as well as mid-gamma within and between both regions.

Furthermore, our analysis of Cross-Frequency Coupling (CFC) in the mPFC demonstrates the presence of at least two distinct pairs of frequency bands for which the amplitude of the higher frequency oscillation (mid- or high gamma) is significantly modulated by the phase of the lower frequency oscillation (delta or theta).

Combined with previous evidence, these results suggest unique mechanisms and functions for each feature of this complex interplay of oscillations in fear learning, retrieval, and extinction. Future experiments are being designed to demonstrate causal links between patterned neural activity and emotional memory, and to translate the analytic approach for clinical use.

Corticolimbic Oscillations in Fear Learning

By

Teresa Emerick Madsen
B.A., Grinnell College, 2004

Advisor: Donald G Rainnie, Ph.D.

A dissertation submitted to the Faculty of the
James T. Laney School of Graduate Studies of Emory University
in partial fulfillment of the requirements for the degree of
Doctor of Philosophy
in
Graduation Division of Biological and Biomedical Science
Neuroscience
2014

Dedications

- To many unspecified members of my family, whose assorted neuroses (in the most loving way possible) have inspired my fascination with the brain.
- To my Dad, George Emerick, for always "making stuff up" when I asked a question you didn't know the answer to – those logical hypotheses introduced me to the scientific method, and I wouldn't be who I am today without that encouragement of my childish curiosity.
- To my Mom, Sally Stovall, for showing me how to live mindfully, according to my values – I'm still striving to emulate you in this.
- To my husband, Jeff Madsen, who has accompanied me on this long journey – right by my side both at the highest peaks of inspiration, aspiration, and pride, and in the lowest valleys of frustration, disillusionment, and despair – for sacrificing to support my ever evolving dreams.
- To my son, Phineas Gage Madsen, for being the light of my life, pure joy, and my favorite distraction – you're totally worth it.

Acknowledgements

The work presented in this dissertation was funded by NIMH R-01 MH069852 and a NARSAD 2009 Independent Investigator Award to DGR. Partial support for TEM was provided by NIDA T32 DA015040 and by the Center for Behavioral Neuroscience (NSF Agreement No. IBN-9876754). Facilities and support services were provided by the Yerkes National Primate Research Center base grant P51RR165/P51OD011132, Animal Resource Program at NIH.

I would like to thank the administrators of the Emory Neuroscience Program, from Sonia Hayden and Yoland Smith to Shawn Hochman and Malu Tansey, for supporting me through a couple more years of graduate school than expected. The hard parts have been smoothed over most effectively by commiseration and companionship with my fellow Emory NS students, including early collaborator John Rolston and labmates – Dave Erhlich, Steve Ryan, Sarah DeWitt Daniel, and Tom Hennessey. Since I've been working on my dissertation from home over the past year, the isolation and drudgery of writing has been greatly reduced by my virtual friends at PhinisheD.org.

Even more integral to the work presented in this dissertation, were the contributions of over a dozen research assistants / trainees (undergraduate volunteers, rotating graduate students, and the occasional post-doc) who came through the lab to learn *in vivo* electrophysiology from me. While some of these partnerships can be most fondly looked back on as managerial learning experiences, I am especially grateful for the two that developed into lasting friendships: Andy Peters and Carmen Collins.

Each member of my dissertation committee – Helen Mayberg, Joe Manns, Kerry Ressler, and Beth Buffalo – deserves special thanks for recognizing my strengths amidst my own focus on the flaws in my work. Their compassionate guidance and encouragement invariably had me leaving committee meetings with a better sense of meaning and direction in my work and far more self-confidence than when I entered.

Finally, my gratitude to Tig Rainnie can't be adequately captured in words. When we met for my very first interview as an Emory Neuroscience recruit, he shared his infectious enthusiasm for the microcircuitry of the amygdala. He took a risk in hiring me for an early summer rotation, and strangely persisted in believing that I would make a good addition to his lab, even after I admitted to having no interest whatsoever in continuing with its primary technique of *in vitro* patch clamp electrophysiology. I insisted on the importance of directly associating neural activity with the ongoing behavior of an awake animal, and he gave me the freedom to explore the possibility of bringing such capabilities to his lab. He miraculously pulled together the funds for an *in vivo* electrophysiology rig, and entrusted me with the task of teaching myself how to use it and of fairly independently running that side of the lab for the next several years. He made sure I had the resources I needed to be successful, connected me with multiple beneficial collaborations, and helped me see the big picture when I got lost in details.

Aside from all the scientific guidance, I think the single most important contribution he made to my development as a scientist has been the unwavering faith he has in me. With the freedom and independence he allowed me, I learned many things the hard way, but now have a deeper understanding than I ever could have gained

secondhand. Building my project from the ground up has given me all the more confidence in my abilities, and a greater sense of accomplishment and pride, that no amount of external praise could come close to matching. Even when nothing was going right and I wasn't sure I'd make it through this, Tig never stopped believing in me, pushing me and encouraging me, but also backing off and trusting me to figure it out myself when I was ready. I cannot thank him enough for his patience and support through the most trying of times. Tig loves his lab like a family, and I hope he knows we love him like a father in return.

Table of Contents

1. Introduction

1.1. Motivation: Neuropsychiatric Disorders

Mental illness is extremely widespread, with current incidence estimated at one in four US adults and lifetime prevalence approaching 50% (Reeves et al., 2011). Among developed nations, mental illnesses account for more time lost to disability than any other category of disease. The economic burden—including lost wages, government disability benefits, and health care costs—has been estimated at $300 billion per year for the US alone (Reeves et al., 2011). In contrast to recent medical advances in the prevention, treatment, and cure of infectious diseases and other obviously physical ailments, the field of psychiatry seems largely stagnant over the past 25 years (Insel and Landis, 2013). While some novel antipsychotic and antidepressant medications have been developed, there has been no corresponding reduction in morbidity or mortality, likely because the drug targets have not been based on any concrete information on the underlying mechanisms of disease (Insel and Landis, 2013). However, a growing appreciation of the brain circuit dysfunctions underlying these "neuropsychiatric disorders," as they are increasingly referred to, has led to the promise of objective biomarkers and novel treatment approaches.

1.2. Corticolimbic Processing of Emotion

In neuropsychiatric disorders that primarily impact emotion, such as the two most common categories – mood and anxiety disorders – the brain circuit that is disrupted tends to be the corticolimbic system. Responsible for the processing of both negative (*e.g.*, sadness, fear, anxiety) and positive (*e.g.*, happiness, reward, motivation) components of emotion, this circuit includes the amygdala, hippocampus, and a number of related structures, including thalamic nuclei and both frontal and temporal cortical areas. To study "emotion" in rodents, a popular paradigm has been Pavlovian fear conditioning, in which a neutral conditioned stimulus (CS, *e.g.*, a novel tone) comes to elicit a conditioned fear response (CR, *e.g.*, freezing) after being paired repeatedly with an intrinsically aversive unconditioned stimulus (US, *e.g.*, a mild footshock). Subsequent extinction, by which the CS no longer evokes the CR after being presented repeatedly without reinforcement by the US, is known to be a new memory of safety that suppresses the expression of, but does not erase, the fear memory.

The basic molecular, cellular, and circuit-level mechanisms of this simple form of emotional learning, along with its utility as a translational model for human anxiety disorders, have been extensively reviewed in recent years (Herry et al., 2010; Pape and Paré, 2010; Milad and Quirk, 2012; Orsini and Maren, 2012; Courtin et al., 2013; Marek et al., 2013; Maroun, 2013; Parsons and Ressler, 2013; VanElzakker et al., 2013). For the purposes of this dissertation, I will focus primarily on the basolateral complex of the amygdala (BLA) and the medial prefrontal cortex (mPFC) and on their dynamic interactions during fear acquisition, expression, and extinction.

1.2.1. Anatomy and Connectivity

The neural structures involved in fear memory are evolutionarily well conserved, due to the ubiquitous drive for self-preservation in the face of danger (Marek et al., 2013). Located in the temporal lobe, the amygdala is a collection of subcortical nuclei that receive multi-sensory input from the thalamus and cortex, associate it with appropriate motivational valence based on memory of past experiences, and trigger behavioral responses via projections to brainstem nuclei (Davis et al., 1994). The basolateral complex of the amygdala (BLA) is the region most strongly linked to the associative learning processes that underlie fear conditioning (Marek et al., 2013). Its intrinsic microcircuitry will be discussed in **Section 1.2.3** below.

The BLA has strong reciprocal connections with the medial prefrontal cortex (mPFC), a region whose roles in fear learning and extinction have historically been much harder to elucidate (Marek et al., 2013). It is composed of at least two subdivisions, the prelimbic (PrL) and infralimbic (IL) cortices, which are thought to have opposing influences over fear learning, despite both sending exclusively glutamatergic projections to the amygdala (Marek et al., 2013).

1.2.2. Roles in Fear Conditioning and Extinction

Sensory inputs from all modalities converge in the BLA, allowing it to form associations between them via synaptic plasticity (Marek et al., 2013). Indeed, NMDA-dependent plasticity in the BLA is necessary for the consolidation of both fear and extinction learning (Marek et al., 2013). Recent evidence suggests that there are two distinct populations of PNs that mediate these opposing forms of memory and can be

distinguished by their projection targets (Senn et al., 2014). That is, BLA to PrL PNs are active during high fear states and diminish their firing upon extinction, while BLA to IL PNs become active after extinction training. Furthermore, optogenetic excitation or inhibition of these two populations bidirectionally altered the consolidation of extinction memories, demonstrating a clear causal link (Senn et al., 2014). However, the dynamic interactions that trigger synaptic plasticity during learning are still only beginning to be understood. Such mechanisms will be explored in more detail in the following sections.

1.2.3. Microcircuitry of the BLA

In spite of its lack of layered organization, the BLA is considered a "cortical-like" nucleus, due to similar cell-types, distributions, and intrinsic connectivity (Ryan et al., 2012). Specifically, approximately 80% of the neurons in the BLA are glutamatergic, pyramidal, projection, principal cells (PNs; Rainnie et al., 1991a), while the other 20% are a heterogeneous mix of GABAergic, inhibitory interneurons (INs; Rainnie et al., 1991b). Burst-firing, parvalbumin positive (PV+) GABAergic interneurons are linked via gap junctions into a syncytium that triggers rhythmic compound inhibitory post-synaptic potentials (IPSPs) in the PNs (Mascagni et al., 2009). In an acute brain slice preparation, the spontaneous rhythm of these IPSPs is around 0.5-4 Hz, but their frequency is modifiable by serotonergic (Rainnie, 1999) or dopaminergic (Muly et al., 2009) signaling. This powerful rhythmic inhibition, delivered via perisomatic basket contacts (McDonald et al., 2005), interacts with the PN's modifiable resonant frequency of 4-5 Hz, at which synaptic input is potentiated (Ryan et al., 2012).

Furthermore, activation of the cAMP-PKA signaling cascade in PNs (*e.g.*, by dopamine D1 receptor agonists) uncovered a 4-6 Hz subthreshold membrane potential oscillation (MPO), which was further amplified after inhibition (Ryan et al., 2012). The interaction of these three convergent rhythms in BLA PNs produced improved spike timing precision and synchrony, which are important for spike-timing-dependent plasticity (STDP), a form of synaptic plasticity that may underlie associative learning (Ryan et al., 2012). Furthermore, theta burst stimulation of afferent inputs into the BLA induces robust long-term potentiation (LTP) in a dopamine D1 receptor dependent manner (Li et al., 2011), which is believed to be a critical substrate of fear learning (Orsini and Maren, 2012).

Thus, the Rainnie lab has demonstrated that the intrinsic circuitry of the rat and primate BLA is optimally set up to facilitate synchronous oscillatory activity in PNs, particularly in the delta (1.5-4 Hz) and theta (4-10 Hz) frequency bands (Ryan et al., 2012). Other labs have found that the isolated rat BLA is also capable of producing beta (10-30 Hz) and gamma (30-80 Hz) oscillations when GluR5-containing kainite receptors are activated *in vitro* (Sinfield and Collins, 2006; Randall et al., 2011). The network of reciprocal connectivity with local INs serves to entrain the membrane potential oscillations of hundreds of PNs, each of which may fire only sporadically, but phase-locked with the population gamma rhythm, allowing the spontaneous formation of cell assemblies. These synchronous cell assemblies, in turn, converge upon downstream targets, which can then integrate the heavy barrages of simultaneous excitatory post-synaptic potentials (EPSPs), likely phase-locking with and powerfully influencing the target region's oscillatory activity (Buzsáki and Wang, 2012). Indeed, such coherent

organized activity is now recognized as a common feature of all cortical-like brain structures and has been implicated in a wide variety of sensory, cognitive, and executive functions, as reviewed in the following sections.

1.3. Neural Oscillations

Coordinated activity among nearby neurons allows for the summation of many transmembrane currents into a measurable extracellular field that reflects the behavior of large populations of neurons (Buzsáki et al., 2012). Depending on the position and properties of the electrode(s) used, recordings of these extracellular potentials are variously referred to as EEG (electroencephalogram, from low impedance electrodes on the scalp), LFP (local field potential, from small implanted electrodes), or spikes (action potentials from one or more neurons in the immediate vicinity of a high impedance microelectrode). Another non-invasive tool, popular for human research due to its higher spatial resolution, is MEG (magnetoencephalography), which measures the magnetic fields produced by these same electrical events (Buzsáki et al., 2012).

At any given recording site, the LFP represents the "spatial average" of all transmembrane currents, weighted by the proximity of source and electrode (Buzsáki et al., 2012). Substantial contributions to the LFP are thought to be made primarily by summated synaptic activity, but also by action potentials and their afterhyperpolarizations, Ca^{2+} spikes, and resonant membrane potential oscillations. Regardless of the specific current source, most individual ionic events would not be

visible in the LFP – synchrony within an appropriate temporal scale across a population of nearby neurons is a key factor contributing to the net magnitude of deflection observed in the LFP (Buzsáki et al., 2012).

Indeed, complex patterns of self-organizing network oscillations are ubiquitous features of brain activity, and they are evolutionarily conserved, in that the spectral features of the EEG or LFP are similar across all mammals (Buzsáki and Watson, 2012). These consistent patterns include a background of chaotic "pink noise" for which the power spectrum is proportionate to the inverse of frequency ($1/f^n$), overlaid with a number of oscillatory bands that are variable in strength and regularity across brain regions and cognitive-behavioral conditions but have been observed to peak around integer powers of *e* (Buzsáki and Draguhn, 2004). That is, $e^1 = 2.7$, in the delta range (δ, 1.5-4 Hz); $e^2 = 7.4$, in the theta range (θ, 4-10 Hz); $e^3 = 20$, in the beta range (β, 10-30 Hz), and $e^4 = 55$, in the gamma range (γ, 30-80 Hz). Each of these bands corresponds to a different scale of temporal integration, originating from distinct cellular and molecular mechanisms, and serving unique functions.

The consistent observation of peaks in these same frequency bands across disparate species is particularly significant given the architectural changes – including more efficient myelination of longer axons and the increasingly folded cortical mantle – that must have evolved to maintain nearly identical temporal patterns in brains that differ by up to 1000x in volumetric scale (Buzsáki and Watson, 2012). Such evolutionary conservation is a testament to the significant role of temporal coding in neural computations. One notable exception is the hippocampal theta rhythm, which is fastest

(6-12 Hz) in rodents and slows down to accommodate longer conduction delays in larger brains (4-6 Hz in carnivores and 1-4 Hz in humans).

However, one consistent underlying principle of all neural oscillations is that they can effectively bias incoming information to be either amplified, if synaptic input arrives during a receptive phase, or ignored, if an input of the same strength is received during a phase of suppressed responsivity (Uhlhaas and Singer, 2012). All known neural oscillations are based on the rhythmic inhibition of projection neurons, such as the spontaneous pattern of BLA activity observed *in vitro* and described in **Section 1.2.3**. The various frequencies arise from the interplay of the biophysical properties of individual neurons, setting up different preferred resonant frequencies in each cell type, and complex network interactions that arise out of the unique connectivity patterns between these cell types (Wang, 2010). The cellular resonance frequencies can be influenced differentially by multiple conductances with unique time constants, including both glutamatergic and GABAergic synaptic activity, gap junctions, neuromodulator-triggered intracellular signaling cascades, voltage-activated currents, membrane capacitance, and passive "leak" currents. Furthermore, multiple neuromodulatory systems are capable of influencing the different patterns of oscillation and synchrony (Uhlhaas and Singer, 2012).

1.3.1. Gamma Mechanisms & Functions

The most thoroughly studied and understood neural oscillation, both in terms of mechanisms and functions, is the gamma frequency band (30-80 Hz), which is known to operate very similarly in the neocortex, hippocampus, and other cortical-like structures

such as the amygdala (Buzsáki and Wang, 2012). Parvalbumin-positive GABAergic interneurons (PVINs) are critical for the production of gamma oscillations in the LFP, as they are capable of continuous firing at 200 Hz or more without fatigue, have a resonant frequency preference in the gamma range, and are the only cell type found to spike on nearly every cycle of the concurrent population gamma rhythm (Sohal, 2012). Furthermore, their perisomatic basket-style innervation of projection neurons produces powerful inhibition, mediated by GABA-A receptors, which can have different subunit compositions that alter the time constant and thus influence gamma frequency.

Indeed, two recent optogenetic studies demonstrated that rhythmic activation of PVINs, but not of PNs, could drive network oscillations in the gamma range (30-60 Hz) but not at any of the higher or lower light pulse frequencies tested (Cardin et al., 2009). Conversely, a single light pulse to activate PNs triggered a brief gamma oscillation, but this evoked gamma power was significantly reduced by simultaneous optical suppression of PVINs (Sohal et al., 2009). *In vivo*, the PVINs take an irregular excitatory drive mediated by AMPA and NMDA receptors and output rhythmic inhibition to entrain network activity (Uhlhaas and Singer, 2012). This delicate balance of excitation and inhibition in microcircuits composed of reciprocally connected PNs and PVINs forms the basis of neural computation.

Synchronization of distant cortical modules is mediated primarily by glutamatergic projections that synapse on both PNs and PVINs, providing a short window of excitation that is quickly shunted by feedforward inhibition. If such afferent input is strong enough, it can reset the phase of the receiver's local oscillations to match

that of the sender. This is a particularly flexible and energy-efficient mode of information transfer between cortical modules (Buzsáki and Watson, 2012).

The importance of gamma frequency in particular comes from its ability to coordinate cell assemblies within the timescale necessary for integration of synaptic inputs and for spike-timing dependent plasticity, which requires temporal precision within the width of a gamma oscillation (10-30 ms) (Dan and Poo, 2006). Gamma frequency synchronization is now thought to play a major role in attention, multi-sensory integration, motor planning, learning, and memory, and synchronized oscillations are recognized as a ubiquitous mechanism by which the brain can bind distributed neuronal activity (Klimesch et al., 2010). A detailed accounting of its functional involvement in the numerous perceptual, cognitive, and executive processes with which gamma synchrony has been correlated would be beyond the scope of this dissertation. However, evidence for the involvement of gamma in motivation and emotion, and for its disruption in neuropsychiatric disorders, will be presented in **Section 1.4**.

1.3.2. Theta Mechanisms & Functions

Theta, on the other hand, has been extensively studied primarily in the hippocampus, where it is entrained by rhythmic input from the medial septum (MS) but also emerges spontaneously from isolated portions of the hippocampus *in vitro* (Colgin, 2013). There appear to be multiple theta oscillators that vary in mechanism and frequency preference along the length of the hippocampus, but all are mediated by interactions between pyramidal cells and inhibitory interneurons. Thus, the mechanisms of theta rhythmogenesis are likely similar to gamma, as described in the previous section, but influenced by conductances with longer time constants, such as spike

afterhyperpolarizations, and hyperpolarization-activated and cyclic nucleotide-gated nonselective cation (HCN) channels (Colgin, 2013).

Theta oscillations in the hippocampus are particularly known for their role in spatial navigation and memory. They organize the firing of place cells, which represent overlapping locations in a familiar environment, into sequences that reflect where the animal has recently been, where it is currently, and where it is planning on going, each firing at a different phase of the ongoing theta oscillation (Colgin, 2013). A given place cell fires at a progressively earlier phase of theta as the animal moves through the corresponding location, a phenomenon known as "theta phase precession." Intriguingly, the sequence of place cells fired while the animal travels a path is, under various circumstances, replayed at different speeds and sometimes in reverse. This repetition of firing sequences, especially during sleep, is thought to contribute to synaptic plasticity, and thus, to memory consolidation (Colgin, 2013). Furthermore, each place cell is phase-locked to a gamma oscillation nested within each theta cycle, and overlapping place cell fields fire within the excitable phase of the same gamma cycle, forming a cell assembly (Lisman and Jensen, 2013). More on this cross-frequency coupling will be discussed in **Section 1.3.3**.

It is well known that the mPFC synchronizes with hippocampal theta during working memory tasks and anxiety-like behaviors (Colgin, 2011). The emotional memory related coherence involving the mPFC and/or the amygdala will be discussed in more detail in **Section 1.5.1**. Mechanistically, the mechanisms of theta entrainment of distal brain regions are similar to those described above for gamma – glutamatergic projections onto PNs combined with feedforward and/or feedback inhibition from local

interneurons (Hartwich et al., 2009; Bienvenu et al., 2012) – except that, given the longer period of a theta cycle (~150 ms), there is more time spent in the activation-favorable phase to allow for longer conduction and multiple synaptic delays, potentially recruiting neurons within a larger volume of tissue into the theta rhythm (Colgin, 2011). As with gamma, the theta cycle represents alternating periods of excitability and suppression, leading to LTP or LTD of synaptic inputs arriving at different phases (Hyman et al., 2003; Albers et al., 2013). However, one of its most critical functions may be its phase modulation of gamma, as introduced above and discussed in more detail in the following section.

1.3.3. Cross-Frequency Coupling Mechanisms & Functions

When multiple oscillations at different frequencies are present, as is often the case, the phase of a slower rhythm often modulates the amplitude of a faster rhythm – a phenomenon known as cross-frequency coupling (CFC). This establishes a hierarchical organization of neural oscillations, similar to the syntactical relationships in all languages between letters or phonemes, words, and sentences (Buzsáki and Watson, 2012). For example, hippocampal theta phase modulation of cortical gamma power parses the gamma oscillations into short "words" which may contain sequential activations of cell assemblies nested as "letters" within each gamma cycle. This biases the feedback from cortical computations to arrive during a specific receptive phase of the ongoing theta oscillation. The slower oscillations detectable in fMRI and described as "default mode" activations may similarly group theta oscillations into "sentences." Each nested oscillation serves to group related information into functional "packets" that can be

integrated by “reader” neurons and interpreted as single events (Buzsáki and Watson, 2012).

As a rule, faster oscillation frequencies mean narrower time windows available for signals to summate and be detected in the LFP (Buzsáki and Watson, 2012). Compared to the relatively slow conduction speed of action potentials along axons, this limits the volume of brain tissue that can be directly involved in the production of a gamma (or faster) rhythm. Slower rhythms, such as delta and theta, on the other hand, have sufficient time to recruit large networks into a coherent oscillation. Thus, CFC allows fast local computations to be linked with similar processes in distal brain regions via the slower phase modulation, allowing integration of information across multiple spatial and temporal scales (Uhlhaas and Singer, 2012).

While the behavioral and cognitive readouts of neuronal activity in the amygdala and prefrontal cortex are not nearly so precisely understood and easily interpreted as the hippocampal place cell coordination described previously (Lisman and Jensen, 2013), the evidence suggests that all cortical-like microcircuits probably use similar mechanisms to bind or “chunk” related information into each cycle of theta (Canolty and Knight, 2010).

1.3.4. Motivation and Emotion in Human EEG/MEG

Affective processes may also utilize a similar binding phenomenon as the mechanism associating neutral stimuli with motivational or affective salience. Indeed, an intracranial recording study in epileptic patients proposed that increased gamma power (30-50 Hz) oscillations in the amygdala, seen when subjects viewed aversive pictures, but

not pleasant or neutral ones, represents an emotional binding function (Oya et al., 2002). The cortical EEG of drama students intentionally re-experiencing emotional memories from their pasts displayed stronger spectral correlations in delta (1-4 Hz) during fear and in both alpha (8-13 Hz) and high beta (20-30 Hz) during anger (Rusalova and Kostyunina, 2004). A human magnetoencephalogram (MEG) study showed an increase in theta oscillations (5-8 Hz) in the left amygdala in response to negative but not positive words using a linguistic affective priming task (Garolera et al., 2007). Prefrontal theta oscillations during REM sleep have been implicated in the consolidation of human emotional memory (Nishida et al., 2009).

Knyazev (2007) reviewed a mix of animal and human data to conclude that delta oscillations are related to motivation and salience detection, whereas theta contributes to memory and emotional regulation. Alpha, which was inversely correlated with the two lower ranges and thought to be increasingly important over the course of evolution and of human development, is involved in the prefrontal inhibitory control of motivational and emotional drives that is necessary for cognitive functions such as selective attention (Knyazev, 2007). Examples of causal links between human emotion and neural oscillations, wherein specific oscillatory differences have been found to underlie affective disorders, will be reviewed in the following section.

1.4. Dysrhythmias / Oscillopathies

Remarkably, nearly every major category of mental illness – including psychotic disorders, anxiety disorders, mood disorders, addictive disorders, autism spectrum

disorders, attention deficit disorders, and personality disorders – has been associated with one or more disruptions of these critical dynamic neural systems (Buzsáki and Watson, 2012). In fact, there has been a lot of recent interest in the use of EEG and/or MEG to identify the oscillatory "fingerprints" of each neuropsychiatric disorder, opening the possibility of clinical uses for differential diagnosis, treatment response prediction, and even direct modification as a therapeutic approach (Williams and Sachdev, 2010; Buzsáki and Watson, 2012; Uhlhaas and Singer, 2012).

For example, depressed patients have shown stronger alpha (8-12 Hz) and beta (10-30 Hz) oscillations than controls, along with an abnormal asymmetry of frontal alpha (Buzsáki and Watson, 2012). In fact, these and other electrophysiological abnormalities can be used to predict whether a patient will respond to typical serotonergic anti-depressants or benefit more from a different treatment option. The related bipolar disorder has been associated with alterations of induced responses in the beta and gamma (30-80 Hz) bands (Buzsáki and Watson, 2012). Indeed, MEG can be used to distinguish between unipolar and bipolar depression, even outside of specific episodes of depression or mania (Williams and Sachdev, 2010). Similar impairments in neural synchrony in schizophrenia parallel its overlap in biological vulnerability with bipolar disorder (Uhlhaas and Singer, 2012). As the best studied example of oscillopathy in neuropsychiatric disease, schizophrenia will be addressed in more detail in **Section 1.4.1**.

In chronic addiction to nicotine or cocaine, stimulus-evoked cravings have been shown to induce an increase in frontal beta (Alcaro and Panksepp, 2011). Likewise, alcoholics exhibit higher resting beta, more alpha synchrony between the hemispheres, and less evoked gamma in visual tasks (Buzsáki and Watson, 2012). Furthermore, their

impulsivity and risk-taking behaviors correlated with reduced anterior theta power during reward processing (Kamarajan et al., 2012). Even personality disorders, some of the most mysterious forms of mental illness, have been associated with abnormalities of alpha and beta rhythms (Buzsáki and Watson, 2012).

Neurodevelopmental disorders, which arise in childhood, also involve dysrhythmias. Compared to controls, people with attention deficit hyperactivity disorder (ADHD) have increased frontal theta, higher ratios of theta to beta power, and a larger gamma response to auditory stimuli (Buzsáki and Watson, 2012). Patients with autism spectrum disorders (ASD) also have a number of altered EEG/MEG patterns, including reduced amplitude and phase-locking of gamma during sensory processing, which likely contributes to the patients' observed impairment in perceptual organization (Uhlhaas and Singer, 2012). Compared to both normally developing toddlers and other forms of language delay, toddlers with ASD showed reduced connectivity between language areas on each side of the brain, which correlated with the severity of verbal and other symptoms. Resting-state oscillations in adults with ASD – including increased theta in the left hemisphere, reduced long-range coherence in the alpha band, and increased local connectivity in the delta band – point toward an imbalance in local vs. global processing (Uhlhaas and Singer, 2012).

1.4.1. Schizophrenia

The best studied examples of oscillopathy come from schizophrenia, which is one of the most pervasively disruptive neuropsychiatric disorders, affecting sensory perception, cognition, and executive control, in addition to emotion (Buzsáki and Watson, 2012). It is also one of the most difficult to treat, with current dopaminergic medications

ameliorating only the positive symptoms (hallucinations and delusions), but not the negative symptoms (*e.g.,* flat affect, anhedonia) or cognitive deficits, which underlie much of the functional disability associated with this disease (Uhlhaas and Singer, 2012). The oscillatory differences that have been noted in patients with schizophrenia include increased delta/theta power in the EEG (Lisman, 2012) and impaired induction of gamma band oscillations in a variety of cognitive and behavioral tasks, which may or may not be due to an increased level of baseline gamma power (Uhlhaas and Singer, 2012). The level of gamma dysregulation correlates with the severity of symptoms, but can also be detected in first degree relatives without a diagnosis of schizophrenia, making it a candidate "endophenotype" that may be more objectively traced to its genetic determinants (Buzsáki and Watson, 2012).

The biochemical basis of this gamma dysrhythmia is already becoming clearer, and in fact, represents a critical demonstration of the importance of GABAergic inhibition, especially from parvalbumin-positive interneurons (PVINs), in the expression of gamma oscillations. Deficient cortical GABA synthesis is a conserved feature of schizophrenia, and this has been linked to a shortage of GAD67 prominent in PVINs (Lewis et al., 2012). Further alterations in the distribution of GABA receptor subtypes and membrane transporters interact with parallel changes in glutamatergic, cholinergic, and dopaminergic innervations to produce a dramatic disruption of the excitatory-inhibitory balance that makes coordinated oscillatory behavior and normal cognition possible (Benes, 2010).

Recent advances in this field have renewed hope of novel biomarkers and therapeutic strategies (Williams and Sachdev, 2010). If susceptible individuals can be

identified during the prodromal period before onset of the first psychotic episode, some form of early intervention may even be capable of altering the developmental trajectory and prevent the full-blown disorder (Uhlhaas and Singer, 2012). These potential improvements in our treatment of schizophrenia should motivate further translational research into the delicate microcircuits that underlie oscillatory neural activity, which is critical for normal cognition, emotion, and motivated behavior.

1.4.2. Anxiety Disorders

While schizophrenia is a dramatic example of oscillopathy in a neuropsychiatric disorder, with a relatively easy to understand etiology, it is not a particularly common disease. Anxiety disorders, on the other hand, afflict approximately 18% of US adults (Reeves et al., 2011). Thus, improved awareness of their etiologies and underlying brain circuit disruptions could lead to new biomarkers and therapeutic approaches that could impact millions of people. Luckily, fear and anxiety are among the few emotions that can be reproduced in rodent models with relatively high construct and face validity (Parsons and Ressler, 2013). Thus, many decades of intense research have already gone into the functional, anatomical, cellular, and molecular underpinnings of fear behavior, anxiety states, and stress effects (see the numerous reviews cited in **Section 1.2**).

Another important feature of animal models is predictive validity, wherein drug responses in the model predict therapeutic efficacy in the human clinical population. Conversely, a clinical benefit can be traced to its biological effectors through a thorough investigation in the model. One pertinent example is the common effect of all known anxiolytics, but not sedatives or other drugs, to reduce the corticolimbic theta oscillations that are evoked by stimulation of the reticular formation in rodents (McNaughton et al.,

2013). A noninvasive human parallel was found in an approach-avoidance paradigm: a 9-10 Hz frontal theta oscillation triggered by this motivational conflict positively correlates with neuroticism and trait anxiety, and was reduced by two different anxiolytic medications with distinct mechanisms of action (McNaughton et al., 2013).

A cross-frequency power correlation between delta and beta bands has also been associated with anxiety. This amplitude-amplitude coupling increases in anxiogenic situations, but is also greater at rest in socially anxious adults. Most interestingly, successful treatment of social anxiety with cognitive-behavioral therapy (CBT) was associated with a decrease in this measure (Miskovic et al., 2011). Biomarkers such as these have the potential to revolutionize the way we diagnose, categorize, and treat neuropsychological disorders. Multiple recent reviews have especially emphasized the value of analyzing a variety of simultaneous electrophysiological measures, including the dynamic, nonlinear associations between different frequency ranges and regions of the brain, both at rest and during relevant tasks (Popov et al., 2012; Schutter and Knyazev, 2012; Uhlhaas and Singer, 2012; Başar, 2013).

1.5. Corticolimbic Oscillations in Emotion

At the time this dissertation project was first proposed and initiated (2007), animal studies were only beginning to demonstrate increased synchrony between the amygdala and the hippocampus or rhinal cortices during emotional memory formation and retrieval. Specifically, gamma band (35-45 Hz) coherence appeared between the BLA and rhinal cortex during the training of an appetitive conditioning task (Bauer et al.,

2007), and synchronized theta activity (4-5 Hz) in the amygdala and hippocampus was observed during the retrieval of fear memory (Seidenbecher et al., 2003; Pape et al., 2005; Narayanan et al., 2007). However, at that time, only one published study had directly investigated synchronization between the amygdala and prefrontal cortex (Stevenson et al., 2007). That experiment was performed in anesthetized rats, a state known to cause an abnormal increase in low-frequency oscillatory activity and neuronal synchrony (Steriade et al., 1993), and hence the results must be interpreted with caution.

Regardless, these data strongly suggested that the amygdala uses frequency codes, in the form of synchronous oscillations, to communicate with remote brain regions during emotion-related tasks. Indeed, the earliest of our preliminary studies towards this dissertation project had already replicated and enhanced these results by observing behavioral state dependent, coherent BLA and mPFC interactions in freely moving rats.

Given all of the translational relevance described in the previous section, it should come as no surprise that, in the last seven years, much more work has been done in preclinical rodent studies such as ours to localize sources and examine mechanisms of these emotion-related oscillations, using more invasive recording and stimulation methods. In the next few sections, I will briefly review the concurrent evidence of delta/theta or gamma oscillations in the amygdala, prefrontal cortex, and/or other structures implicated in fear learning. However, even now, no one else has examined the full delta-through-gamma power spectra of both the amygdala and medial prefrontal cortex simultaneously, much less looked at the dynamic interactions between frequencies

over the course of habituation, acquisition, recall, and extinction of Pavlovian conditioned fear.

1.5.1. Delta (1.5-4 Hz) / Theta (4-10 Hz) Frequencies

In parallel with the work described in this dissertation, other groups were also discovering that coherence of theta band oscillations occurs between the medial prefrontal cortex, the amygdala, and the hippocampus during fear recall, and that this activity diminishes over the course of extinction (Sangha et al., 2009). A similar relationship was found between mPFC and hippocampus during the expression of innate anxiety: higher theta coherence for mPFC LFPs and single units with the hippocampal LFP when mice explored the open arms of an elevated plus maze, compared to the relative safety of the closed arms (Adhikari et al., 2010, 2011). Significantly, the strength and directionality of BLA → mPFC theta coherence during bouts of REM sleep after fear conditioning were found to correlate with successful consolidation of the fear memory, expressed by minimal decrease in freezing upon CS presentation the following day (Popa et al., 2010).

In an attempt to demonstrate a causal relationship, Lesting and colleagues (2011) disrupted synchronized oscillations with anti-phase (alternating, 180° apart) theta stimulation of the amygdala and hippocampus and showed that extinction learning was delayed by this manipulation. While they also argued that in-phase (simultaneous) theta stimulation accelerated extinction learning, this was based on a statistical difference from anti-phase stimulation, but not from sham stimulation (Lesting et al., 2011).

In contrast, another lab found that artificial theta stimulation of the hippocampus alone impaired encoding of contextual fear memory (Lipponen et al., 2012). It is unclear whether this latter stimulation effect primarily demonstrates that theta oscillations have a general anti-fear effect, contrary to prior evidence, or more likely, if the disruptive effects of theta stimulation on any form of learning relate to the mixed effects of electrical stimulation on excitatory projection neurons (eliciting both orthodromic and antidromic action potentials) as well as activating local inhibitory interneurons. Furthermore, it could relate to a poor choice of stimulation parameters: Lesting and colleagues (2011) used 5 Hz theta bursts of 200 Hz square wave pulses, similar to the 4-6 Hz patterns they had previously recorded during fear expression in mice, while Lipponen and colleagues (2012) used longer individual pulses delivered at 8 Hz, near the peak frequency of hippocampal theta during exploratory behavior, while the peak frequency of sham operated rats during freezing was approximately 5-6 Hz. Thus, Lipponen's chosen stimulation may have unintentionally biased the corticolimbic network toward locomotion rather than freezing.

Two more comprehensive, yet correlative, studies of corticolimbic theta oscillations have been reported in the past year. The first demonstrated that freezing behavior during fear recall was accompanied by zero-lag theta synchrony between IL-mPFC, CA1, and LA, whereas successful extinction (i.e., non-freezing times during the CS) correlated with IL-mPFC units and LFP maintaining a significant theta phase lead over the LFPs of both CA1 and LA (Lesting et al., 2013). Similarly, Likhtik and colleagues (2014) recorded multiunit activity and LFPs in mPFC, dorsal and ventral hippocampus (dHPC and vHPC, respectively), and BLA of mice upon recall of

differential fear conditioning and during an open field test. In both the learned fear and innate anxiety tasks, behavior indicative of recognized safety (*i.e.,* non-freezing during CS- presentation or exploration of the center of the open field, respectively) was associated with lower theta power and coherence, as well as a higher likelihood of the mPFC leading the BLA in theta phase (Likhtik et al., 2014). This represents the greatest number of simultaneously recorded corticolimbic sites, along with a rare comparison of learned fear and innate anxiety, but no frequencies over 40 Hz appear to have been examined.

Finally, Courtin and colleagues (2014) have recently used sophisticated optogenetic techniques to reveal the most convincing evidence of a causal relationship between corticolimbic theta and fear behavior. They found that optical inhibition of parvalbumin-positive interneurons (PVINs) of the dorsomedial prefrontal cortex (dmPFC, including PrL & AC) disinhibited projection neurons targeting the BLA and triggered a transient power increase and phase-reset of local high theta (8-12 Hz) oscillations. Behaviorally, this manipulation elicited freezing in unconditioned mice, reinstated fear in extinguished mice, and produced place aversion in an active avoidance paradigm. In contrast, optical excitation of dmPFC PVINs prevented this theta phase reset and transiently inhibited freezing when delivered along with a feared CS. Notably, the authors themselves point out that this high theta band was significantly more prominent during exploration and did not spontaneously appear as a peak in the power spectrum during freezing (Courtin et al., 2014).

Thus, it is unclear whether this data can be reconciled with all previous evidence implicating the low theta (4-6 Hz) range in fear learning and expression, or if the low and high theta bands are indeed unique in both mechanism and function. Nevertheless, their demonstration of a causal role for dmPFC PVIN deactivation in fear expression represents exciting new progress in our understanding of the cellular mechanisms of theta phase locking and its relationship to fear (Courtin et al., 2014). However, it still paints an incomplete picture of corticolimbic oscillations, as this study did not include simultaneous recordings throughout the network to determine the downstream effects of their manipulation, nor did they examine any frequencies over 20 Hz, or even outside of the high theta (8-12 Hz) filtered LFP used in the majority of their analyses.

1.5.2. Gamma (30-80 Hz) Frequencies

As mentioned in **Section 1.5**, gamma in the BLA had already been shown to become coherent with the rhinal cortices during appetitive trace conditioning (Bauer et al., 2007). Popescu and colleagues (2009) later extended this finding to show BLA gamma coherence with the striatum while animals were learning which of two stimuli predicted a reward.

Interestingly, until this past year, most of the evidence for gamma involvement in negative emotions and aversive learning had come from human EEG and MEG studies, as described in **Section 1.3.4**. A comprehensive review by Headley and Paré (2013) presented evidence that negatively valenced emotional stimuli elicit increased gamma power in the amygdala and cortex. These gamma oscillations could be either “evoked” (short-latency and time-locked to stimulus onset) or “induced” (with a latency of several hundred milliseconds and no phase-locking across trials). The former responses could be

altered by emotional content even in subliminally presented stimuli, whereas the later represented conscious processing of the emotional stimuli. Furthermore, induced gamma was the most strongly impacted by emotional learning, such as upon retrieval of conditioned fear (Headley and Paré, 2013).

In one of the few animal studies linking gamma oscillations and fear conditioning, the power of auditory cortex gamma induced by the CS+ during the initial acquisition of fear conditioning predicted both plastic changes in tone specificity and later expression of the fear memory (Headley and Weinberger, 2011). Furthermore, repeated CS-US pairings across several days continued to increase the power of induced gamma, specifically at auditory cortex recording sites that were tuned within one octave of the CS tone and less so at sites tuned to frequencies more than an octave higher or lower than that of the CS tone (Headley and Weinberger, 2013). While notable in that these studies include rare recordings during acquisition of fear conditioning, they only investigated gamma activity in the primary sensory area, rather than the corticolimbic circuit.

Finally connecting corticolimbic gamma and fear memory, Courtin and colleagues (2013b) recently demonstrated that gamma oscillations in the BLA were enhanced after fear conditioning and reduced in amplitude over the course of extinction training and retrieval. Furthermore, the ratio of gamma power in late extinction vs. early extinction was significantly predictive of the level of freezing in a retrieval test one week later. That is, mice with stable or increased gamma power between extinction sessions were more likely to demonstrate spontaneous recovery of the fear memory (Courtin et al., 2013b).

To move beyond these observational studies of gamma correlations with learning, another recent paper used optogenetic stimulation at different frequencies. Excitation of glutamatergic BLA projection neurons via 40 Hz, but not 20 Hz, optogenetic stimulation immediately after training on an inhibitory avoidance task was found to enhance consolidation of that memory, as demonstrated by longer latency to enter the shock chamber upon testing the following day (Huff et al., 2013). Conversely, continuous optogenetic inhibition of the BLA for 15 minutes after training, but not for only 1 min or when delivered 3 hours after training, impaired consolidation, resulting in shortened latency to enter the shock chamber, indicative of poor retention (Huff et al., 2013). Thus, externally driven gamma activity in BLA PNs is beneficial for the consolidation of fear learning, and some BLA activity (not conclusively gamma) is required in the 15 minutes immediately post-conditioning for that memory to be consolidated.

In a creative attempt to disentangle the roles of PrL and IL, Fitzgerald and colleagues (2013) recorded activity in both regions, using strains of mice with either intact (B6) or deficient (S1) extinction learning. The continued fear expression in S1 mice during "late extinction" and an "extinction retrieval" session the following day, was accompanied by higher gamma (but not theta) power in the PrL (but not IL) compared to B6 mice. In fact, despite a non-significant difference in freezing during "early extinction," or fear recall, PrL gamma was already significantly higher in S1 mice than in B6 mice at that time point. Indeed, there were no significant differences in either theta or gamma power in either region across the three testing phases (Fitzgerald et al., 2013a). Rather than clarifying the differential involvement of PrL and IL in fear expression and extinction learning, this negative result seems to bring up more questions than answers.

As all previous evidence for gamma involvement in emotional learning had been amygdalocentric, and all prior investigations of prefrontal oscillations underlying fear learning focused primarily on the theta band, the possibility remained that gamma is not normally recruited in the prefrontal cortex in the context of emotional learning. However, the plentiful evidence for mPFC gamma involvement in working memory and in consolidation of long term spatial memory would suggest that is unlikely.

1.5.3. Cross-Frequency Coupling Knowledge Gap

Together, these data strongly suggest that the amygdala uses frequency codes, in the form of coherent oscillations at delta/theta and gamma frequencies, to communicate with remote brain regions during emotion-related tasks, and that this form of coordinated activity is necessary for appropriate learning to occur. However, the dynamic interactions that may occur across frequencies during fear conditioning have not yet been explored. There are a few recent papers that demonstrate behaviorally-relevant cross-frequency coupling in rats: joint VTA & mPFC delta and hippocampal theta phase modulation of VTA & mPFC gamma amplitude and single unit firing activity during a spatial working-memory task (Fujisawa and Buzsáki, 2011), delta-gamma phase-amplitude coupling within corticobasal-ganglia circuits during spontaneous locomotor behavior (López-Azcárate et al., 2013), and theta-gamma coupling in the prefrontal cortex during trace eyeblink conditioning, which is not dependent on the amygdala (Shearkhani and Takehara-Nishiuchi, 2013). Finally, Adhikari and colleagues (2010) noted that mPFC gamma amplitude was modulated by hippocampal theta, but there was no difference in the magnitude of this modulation between familiar environments, open

field, or elevated plus maze. None of these paradigms is considered "emotional memory," nor did any include recordings in the amygdala.

The work presented in this dissertation is intended to deepen our understanding of multiple dynamic interactions that occur during fear learning, using a spectral and cross-frequency approach to the analysis of multi-channel LFP recordings in the BLA and mPFC of freely-moving rats during tone habituation, fear conditioning, and extinction training.

2. Materials and Methods

2.1. Animals and Pre-training

All animal procedures were approved by the Emory Institutional Animal Care and Use Committee. Eight individually-housed, male, Harlan Sprague-Dawley rats were maintained on a restricted diet at approximately 85% of their normal growth curve, starting at 8-10 weeks of age. In order to maintain a baseline level of activity against which to measure freezing behavior as an indication of fear (adapted from Quirk et al., 2000), animals were trained to press a lever for an intermittent food pellet reward (VI-60: variable interval averaging 60 seconds, using ABET II, Lafayette Instruments, Inc.). This operant training and all later behavioral testing and neural recordings occurred in the same modular operant conditioning chamber, 59.7 x 34.3 x 26.35 cm, with aluminum and polycarbonate walls (Lafayette Instruments, Lafayette, IN). The floor of the chamber was made of 0.4 cm diameter stainless steel bars spaced at 1.1 cm. A speaker was mounted on the wall opposite a single lever and food dispenser.

2.2. Surgery

Two-by-four arrays of 50-micron, Teflon-insulated, stainless steel microwires separated by 200-250 microns within rows and 250-500 microns between rows (Neurolinc or Plexon) were implanted, targeting the right BLA (targeting AP -3.0 mm, ML 5.2 mm, DV -8.5 mm relative to bregma at a 6° angle away from the midline) and the

ipsilateral mPFC (targeting AP +2.7 mm, ML 0.5 mm, DV -5.0 mm relative to bregma at a 6° angle toward the midline, Figure 1a). The surgeries were conducted under isoflurane anesthesia (1-3% in O_2), adjusted according to continually monitored responsiveness to foot or tail pinch, and aseptic conditions. Recording arrays were anchored to the skull with stainless steel screws and dental acrylic. A single dose of metacam (2 mg/kg SQ) was administered for post-surgical analgesia, and the rats were allowed one week for post-surgical recovery.

2.3. Fear Conditioning

Standard Pavlovian fear conditioning began only after animals had reached consistent responding in the VI-60 training sessions with the recording headstage plugged in. Here, animals were presented with repeat pairings of a conditioned stimulus, and an unconditioned stimulus. The conditioned stimulus (CS) was a 4 kHz tone played for 30 seconds at 80 dB, with a variable 2-6 minute inter-trial interval (ITI). The unconditioned stimulus (US) was a scrambled footshock delivered to the floor-bars of the cage at 0.5 mA for 0.5 seconds, and co-terminating with the CS (ABET II). An independent VI-60 food reward schedule ran concurrently with all stages of fear and extinction training (**Figure 1A**):

Day 1 – Habituation (10 tones) and Acquisition (7 tone-shock pairs)

Day 2 – Context Extinction 1 (no tones)

Day 3 – Context Extinction 2 (no tones)

Day 4 – Cue Extinction 1 (15 tones) – beginning considered Recall

Day 5 – Cue Extinction 2 (15 tones)

Context extinction sessions were used, as opposed to different contexts for Acquisition and Extinction, because we found in pilot studies that the cues surrounding recording (e.g., location, handling, and the tethered headstage) were too salient to be overcome by any changes in floor or wall coverings. Thus, the rats would invariably freeze when returned to the recording chamber on subsequent days. However, two days of VI-60 bar-pressing for ~1 hour each, with the headstage plugged in, but without any CS presentations, was sufficient for all conditioned rats to stop freezing and return to their previous levels of responding for the food reward.

2.4. Recording

Neural data was collected each day using a Plexon MAP system, including a 20x headstage and a 50x preamp. Signal data was filtered into two bands: 154 Hz – 8.8 kHz to isolate spikes (digitized at 40 kHz), and 0.7 – 300 Hz to isolate LFPs (digitized at 1 kHz). Prior to any further processing, the LFP data was run through Plexon's FPAlignV2 utility, which corrects for uneven phase shifts across frequencies, given a particular headstage and set of preamp filters.

2.5. Histology

At the conclusion of the experiment, rats were deeply anesthetized with sodium pentobarbital (100 mg/kg IP) and transcardially perfused with 0.9% NaCl followed by 10% buffered formalin. Their brains were extracted and immersed in formalin for at least 12 hrs and then transferred into 30% sucrose until they sank. Brains were then sectioned to 50µm on a cryostat, and the slices mounted onto subbed slides and stained with cresyl violet to visualize electrode placement. The ends of the electrode tracks were mapped onto the rat brain atlas (**Figure 1B**).

2.6. Behavioral Analysis

Freezing was quantified using FreezeScan (CleverSys Inc.) analysis of videos time-locked to the neural data (CinePlex, Plexon). Parameters for the automated analysis were set to detect freezing behavior whenever the rat was motionless except for respiration. The "Barpress Suppression Ratio" (BSR), used as a complimentary measure of fear behavior in response to each tone (adapted from Quirk et al., 2000), was defined as: 0 when the rat pressed the lever seeking food reward as much or more during the tone as before it, 1 when there was no bar-pressing (BP) in the 30 second tone period, and (BP before - BP during)/(BP before + BP during) otherwise.

Successful fear recall was defined as meeting each of the following three criteria for at least two of the first three tone presentations in the first cue extinction session: (1) freezing during tones > 50%, (2) increase over pre-tone freezing > 20%, and (3) BSR >

0.5. Criteria for fear extinction were exactly the opposite: (1) freezing during tones < 50%, (2) increase over pre-tone freezing < 20%, and (3) BSR < 0.5, requiring all three criteria to be met for at least two of the last three tone presentations in the second cue extinction session. Rats that failed to meet the criteria for either recall or extinction were excluded from all group averages and statistical tests.

Each behavioral measure was assessed via one-way Repeated Measures ANOVA, with factor Stage (levels: Habituation, Acquisition, Recall, and Extinction) and 3 tones (first 3 of Recall, last 3 of all other stages) as replicates. Any non-sphericity in the data was adjusted by the Greenhouse-Geisser correction, regardless of the outcome of Mauschly's test, which can be unreliable with small sample sizes. Post-hoc comparisons of any significant ($p < 0.05$) effects were made using paired-sample t-tests with Bonferroni adjustments.

2.7. Spectral Analysis of Local Field Potentials

Local field potential (LFP) data were analyzed using custom Matlab scripts and Chronux, an open-source Matlab toolbox (Bokil et al., 2010). Power spectra and coherence were computed using multitaper spectral estimation, a nonparametric method that allows explicit control over the bandwidth parameter, with the option of trading off frequency resolution for reduced variance (Bokil et al., 2007). One representative LFP recording channel in each region was used for most analyses. Three tones were selected to represent each stage of learning, as follows: last three tones of habituation, last three

of acquisition, first three of the first extinction session ("Recall"), and last three of the second extinction session ("Extinction"). Average spectrograms were calculated for each rat, stage, and region, and then normalized (divided) by the time-averaged power spectrum of the baseline period (30s period before tones during habituation), before being averaged together across animals, giving mean power change from baseline in dB. Along with the corresponding coherograms, these normalized spectrograms were calculated with 1.33s sliding windows, shifting by 0.133s (10%), and using 3 tapers for a spectral bandwidth (W) of ±1.5 Hz.

For statistical comparisons, we used 20 non-overlapping segments of 1.33s each, immediately preceding tone onset during the Habituation stage as the baseline for comparisons with all other time (before, during, or after tones) and stage (Habituation, Acquisition, Recall, or Extinction) combinations, which were also each represented by 20 non-overlapping 1.33s segments. Within each rat, a test statistic for each comparison was calculated using the method described in Bokil et al., 2007, as implemented in Chronux with the functions "two_group_test_spectrum" and "two_group_test_coherence." These functions test the null hypothesis of equality for two spectral or coherence estimates, even in cases of unequal bias between groups of different sizes. However, in our comparisons, each "group" of data consisted of 20 time segments * 3 trials * 3 tapers = 180 statistically independent samples. The test statistic has been shown to be distributed as a unit normal when the two population spectra are known to be equal. To address the possibility of non-Gaussian behavior, a multigroup jackknife procedure provided a robust estimate of the variance, free from any assumptions about the underlying distribution of the data (Bokil et al., 2007).

For the most conservative hypothesis testing in the face of multiple comparisons across the range of frequencies, we defined the threshold for significance by the following criteria: The null hypothesis (no difference from baseline) was rejected only at those frequencies for which the test statistic was outside of both the frequency independent (theoretical) and jackknife variance-based (distribution free) confidence intervals, and which constituted contiguous bands whose width was larger than the bandwidth (2*W = 3 Hz). Thus, rather than reporting a p-value for each frequency bin of each comparison, we graphically depict the number of rats demonstrating significant increases or decreases from baseline at each frequency, according to the above criteria.

2.8. Neural Correlates of Behavior

In order to directly correlate freezing behavior with spectral activity, independent of cue-triggered fear, we created, for each rat, a time series of % freezing in 6s bins through the first 45 minutes of the first extinction session (day 4). Likewise, spectrograms for mPFC and BLA and a coherogram between regions were calculated using the same 6s non-overlapping bins. The Matlab function "corrcoef" was used to obtain correlation coefficients for % freezing with each frequency bin of the spectrograms and coherogram, equivalent to the 0 time lag of their cross-correlations, normalized such that the 0 time lag of the auto-correlations were equal to 1. The p-value for each correlation, as output by this same function, was Bonferroni-corrected for multiple comparisons (# of frequency bins * 3, to cover both spectrograms and the coherogram). Correlations that reached significance (adjusted $p < 0.05$) were classified

as positive or negative based on the sign of the correlation coefficient (R), and the number of rats showing positive or negative correlations with % freezing at the same frequency bins were summed. Finally, the correlation coefficients were averaged across rats, irrespective of significance, as a function of frequency, to illustrate the overall pattern of spectral correlates of freezing behavior.

2.9. Cross-Frequency Coupling

Cross-frequency coupling (CFC) was assessed using the Kullback-Leibler modulation index (KL-MI) as defined in Tort et al., 2010. MATLAB functions were custom written for this project based on demonstration scripts offered by Adriano Tort (personal communication, 2008). The general procedure was as follows (steps 1-3 depicted in **Figure 2**):

1) Filter LFPs into a low band (*e.g.*, 2-4 Hz) and a high band (*e.g.*, 50-55 Hz) using the "eegfilt" function from EEGLAB, which runs the same filter on the data forwards and backwards to correct the phase shifts that occur with only one pass (Delorme and Makeig, 2004).
2) Extract phase information from the low band and the amplitude envelope from the high band, using the Hilbert Transform.
3) Calculate the average gamma amplitude within each of 18 low frequency phase bins (*N*). Record the phase of the low frequency band at which gamma amplitude is maximal for later analysis of phase preference.

4) Compare phase-amplitude distribution (*P(j)*) to the uniform distribution using the Kullback-Leibler distance (the derivation of this modulation index equation can be found in Tort et al., 2010):

$$KL\text{-}MI = \frac{log(N) + \sum_{j=1}^{N} P(j) * log[P(j)]}{log(N)}$$

5) Convert computed KL-MI into a Z-score by comparison with the distribution of KL-MIs calculated from 100 surrogate gamma amplitude envelope time series, produced by the shuffling method defined in Hentschke et al., 2007, which maintains the same frequency components of the original signal while eliminating all phase information.

For each rat, stage of fear learning and extinction, and relative time period (before, during, or after tones), we calculated this CFC z-score across independently sliding frequency bands for both the phase (2 Hz wide bands, with 50% overlap, between 1 & 14 Hz) and amplitude (5 Hz wide bands, with 50% overlap, between 15 & 115 Hz) time series. Significance was tested independently for each rat, after which the number of rats showing significant modulation in each pair of frequency bands was summated. For an overall picture of the strength of modulation between frequency pairs across stage and time, the z-scores for each bin, irrespective of significance, were averaged across all 5 rats that met the behavioral criteria for both fear acquisition and extinction. When calculating average phase preference, however, only those rats' data that showed significant coupling in each bin were averaged (using the function "circ_mean" from the CircStat toolbox, Berens, 2009), so that the random peak phase bin of a signal that was

not significantly modulated would not add noise to the consistent phase relationships seen with significant coupling.

3. Results

3.1. Histology

In all eight implanted rats, the electrodes targeting medial prefrontal cortex consistently hit their mark, with the majority falling in infralimbic cortex, but some anterior contacts in anterior-ventral prelimbic and a small portion of medial orbital cortex, (**Figure 1B**). On the other array, the majority of electrodes landed within the basolateral complex of the amygdala, while others hit more lateral structures including the piriform cortex and dorsal endopiriform nucleus. The recordings revealed a number of highly significant changes in oscillatory neural activity, in both target regions, that were dramatically modulated by the emotional and behavioral state of the animal across stages of learning.

3.2. Behavior

Of the eight rats trained and implanted with electrodes, five successfully learned both the fear and extinction as evidenced by following the expected trajectory of both freezing behavior and barpress suppression ratios (BSR, **Figure 1C**). The three outliers (one that failed to meet criteria for fear recall, one that failed to meet criteria for fear extinction, and one that lost its headcap before the first extinction session) were excluded from all group averages and statistical tests.

The barpress suppression ratio (BSR) was low during habituation, except for the first tone, which was a novel stimulus at the time. As expected, BSR increased sharply during acquisition – that is, all rats stopped barpressing completely after a few shocks. In the first extinction session, the initial fear recall triggered very high BSRs, which then declined with subsequent tone presentations. There was some spontaneous recovery of tone-cued fear measured by the BSR on the following day, but it sharply declined and stayed low – that is, the rats continued barpressing through the tone presentations for the remainder of the second cue extinction session. A one-way repeated measures ANOVA was calculated based on 3 tones per Stage (first 3 for Recall, last 3 for Habituation, Acquisition, and Extinction). The results showed a significant within-subjects effect of Stage on BSR, $F(2.56, 10.239) = 239.576$, $p < .0005$. Post-hoc pairwise contrasts, made using the Bonferroni correction for multiple comparisons, demonstrated that BSR during both Acquisition (1.000 ±0.000, *i.e.*, full suppression for all 5 rats across the last 3 tones) and Recall (0.927 ±0.047) were significantly different from Habituation (0.068 ±0.053) as well as Extinction (0.091 ±0.035, all p-values < .0005), while Acquisition was not significantly different from Recall (p > .9995), nor was Extinction different from Habituation (p > .9995).

Freezing behavior during the tones followed a similar trajectory to BSR, but declined faster (and less variably) during extinction. Mauschly's test indicated that the assumption of sphericity had been violated, $\chi^2(5) = 12.239$, $p = .042$; therefore, degrees of freedom were corrected using Greenhouse-Geisser estimate of sphericity ($\varepsilon = .377$). The results showed that Stage had a significant within-subjects effect on percent of time spent freezing during the tones, $F(1.132,4.528) = 47.516$, $p = .001$. Just like BSR, the post-hoc

tests demonstrated that percent freezing during Habituation (0.873 ±0.370%) and Extinction (6.547 ±2.933%) was significantly less than during Acquisition (63.832 ±9.619%, $p = .017$ vs. Habituation and $p < .0005$ vs. Extinction) and Recall (75.153 ±3.665%, $p = .001$ vs. Habituation and $p < .0005$ vs. Extinction), while there were no significant differences within those pairs ($p > .9995$ for both contrasts).

Tone-specific increases in percent freezing (percent during tone - percent before tone, or 0 if negative) declined more abruptly and consistently than percent freezing (data not shown). Here, the repeated measures ANOVA again showed a significant effect of Stage on increased freezing in response to tones, $F(1.408, 5.632) = 25.243$, $p = .002$. However, the post-hoc comparisons demonstrated a slightly different pattern, in which only Recall (47.007 ±8.626% more freezing during vs. before tones) was significantly greater than all the other stages (Habituation, 0.520 ±0.323%, $p = .038$; Acquisition, 5.767 ±3.876%, $p = .034$; Extinction, 4.113 ±1.551%, $p = .027$). No significant differences were found between the other 3 stages (Habituation vs. Acquisition, $p > .9995$; Acquisition vs. Extinction, $p > .9995$; Habituation vs. Extinction, $p = .607$). In other words, the rats were freezing continuously during Acquisition, so a tone-triggered increase in freezing was not detectable. Only during Recall was the fear behavior truly a conditioned response to the tone.

3.3. Spectral Analysis

Having established tone specific alterations in freezing and BSR during fear acquisition and extinction, we next examined the neural data to determine if any concurrent alterations occurred in the power spectra of local field potentials in the mPFC and BLA. A representative example of the analysis of an LFP recorded in the mPFC during fear Recall (in response to the first tone exposure after fear conditioning) is illustrated in **Figure 3**: The shift from disorganized activity before the tone (blue traces) to a strong, low frequency oscillation during the tone (red traces) was apparent even in the raw data (**Figure 3A**), and became even more obvious in the autocorrelations (**Figure 3B**). To quantify the difference, multi-taper spectral estimation was used to transform each time series into the frequency domain, giving power spectral densities with 95% confidence intervals (**Figure 3C**). As illustrated, fear conditioning resulted in a marked decline in high theta power and a sharply tuned increase in delta power. The inset is a representative spectrogram of the same data, using sliding windows of time to show the rapid and dramatic increase in power and tuning at 2-4 Hz when the tone comes on (t = 0s). Finally, Bokil's spectral statistical test (described in methods, after Bokil et al., 2007) demonstrated a significant difference between test conditions at this single trial level for both the increase in high delta / low theta band (solid arrowhead) and a decrease in high theta (open arrowhead, **Figure 3D**).

We next examined the effects of fear conditioning on neural activity in the mPFC and BLA. For each rat meeting the behavioral criteria for successful fear conditioning and extinction (n=5), the spectrograms of three trials per stage were averaged and divided

by that individual's pre-tone spectrum during habituation, before these normalized spectrograms were averaged across rats. Thus, the resulting spectrograms (**Figure 4A&B**) represent the mean power spectral differences from baseline in decibels. As coherence is inherently a normalized measure, limited to the range of 0 to 1, we did not divide by any baseline factor (**Figure 4C**). These spectrograms will be described in parallel with the corresponding statistics, as described in the next paragraph.

Due to inter-animal variability in both the frequency and absolute level at which the power spectra peaked during fear expression, standard statistical analysis for comparing grouped average power or coherence within pre-determined frequency ranges was not well suited to this dataset. Consequently, we repeated Bokil's statistical test for spectral differences, from before to during tones, within each rat and counted the number of rats demonstrating significant increases or decreases in each frequency band, in each stage of fear and extinction learning (**Figure 5**). For a clearer depiction of the average magnitude of change across rats, the count of increases and decreases is overlaid by the mean test statistic used for these comparisons (green line). In the following textual summary, we will report the frequency ranges in which at least two rats demonstrated significant changes in the same direction.

3.3.1. Habituation

As expected, the Habituation stage showed no tone triggered activity in either the mPFC or the BLA (**Figure 4A&B, left column**), with no obvious peaks in the power change spectra at any of the frequencies measured (1 – 100 Hz), suggesting that tone alone failed to modulate the LFP in either of these limbic regions before the animal

formed an emotional association. However, a baseline pattern of coherence existed between the mPFC and BLA (**Figure 4C, left column**), with delta (<5 Hz) and gamma (50-70 Hz) frequency ranges predominating throughout Habituation (before, during, and after tones). Thus, while a few narrow gamma bands showed spurious increases or decreases in the mPFC power, BLA power, or coherence of only one rat, no consistent patterns of tone-response were observed (**Figure 5, left column**).

3.3.2. Acquisition

In contrast, dramatic changes were apparent in the 2-5 Hz and 30-90 Hz bands of the power spectra of both regions during the last few trials of Acquisition (**Figure 4, left center column**). Beginning with the lowest frequency ranges, the tone was seen to trigger a strong increase in delta band power, together with a decrease in the adjacent 1 Hz and 6 Hz frequency bands, in both BLA and mPFC, and in coherence between them. The delta increase was significant for 4 out of 5 rats in mPFC power, 2 of 5 in BLA power, and 3 of 5 in mPFC-BLA coherence (**Figure 5, left center column**). Importantly, after the US presentation, delta power remained elevated for >30 seconds.

A decrease in higher theta (6-10 Hz) power is visible in the spectrograms of both regions throughout the Acquisition stage (**Figure 4A&B, left center column**). However, as this decrease from the pre-Habituation baseline was apparent in mPFC power even before the Acquisition tone onset (*i.e.*, >90 seconds after the previous shock), it reached significance in the before vs. during tone comparison for only 1 of the 5 rats (**Figure 5, left center column, top row**). In BLA power, 2 of 5 rats showed a significant tone-related decrease in this high theta band (**Figure 5, left center column, middle row**). A

significant decrease in high theta coherence was only detected for 1 of 5 rats (**Figure 5, left center column, bottom row**).

Unexpectedly, we also observed an increase in low beta band (13-17 Hz) power in the mPFC, BLA, and coherence, specifically after the footshock in the Acquisition stage (**Figure 4, left center column**). As this change was exclusive to the post-footshock period, it did not reach significance in any of the before vs. during tone comparisons (**Figure 5, left center column**).

Activity in the gamma frequency range could be divided into three sub bands: low gamma (30-45 Hz), mid gamma (45-60 Hz), and high gamma (60-100 Hz), based on their differential expression in the two target regions and correlated power changes within regions (data not shown). Low gamma showed increased power during the Acquisition stage exclusively in the BLA, after footshocks (**Figure 4B, left center column**). Mid-range gamma was expressed in both regions at elevated levels throughout Acquisition, including before tones (*i.e.,* >90s after the previous footshock), with a notable increase at tone onset and especially after the presentation of the footshock (**Figure 4A&B, left center column**). Coherence in this frequency band dramatically increased after the footshock in Acquisition (**Figure 4C, left center column**). Finally, high gamma was expressed primarily in the mPFC, where an increase could be seen at tone onset and after the footshock during Acquisition (**Figure 4A, left center column**).

In the before- to during-tone comparison, up to 3 of the 5 rats showed significant increases in high gamma power in the mPFC (**Figure 5, left center column, top row**). However, no more than 1 of 5 rats showed significant changes in low or mid-gamma in

mPFC power or any gamma frequency in BLA power or mPFC-BLA coherence (**Figure 5, left center column**). That is, the most dramatic gamma changes occurred after the footshock, rather than at tone onset, as was true of the delta shift. This may reflect differential roles of those oscillatory bands in the fear memory encoding process vs. the simple expression of fear.

3.3.3. Recall

In the fear Recall stage, the delta power increase became even more sharply tuned and was clearly tone triggered (**Figure 4, right center column**). The before vs. during tone comparison demonstrated a significant increase in mPFC power for 3 out of 5 rats (**Figure 5, right center column, top row**). However, only 1 in 5 rats showed significant delta increases in BLA power or mPFC-BLA coherence (**Figure 5, right center column**).

In the spectrograms (**Figure 4, right center column**), the decrease in high theta power became more pronounced in Recall than in Acquisition. However, since it was similarly continuous throughout the 90s trial period, the level of significance in the before vs. during tone comparison was similar: 1 of 5 rats showing a significant decrease in mPFC theta power and 2 of 5 in BLA theta power (**Figure 5, right center column**). Interestingly, coherence between the two regions showed the opposite effect: 2 out of 5 rats showed a significant increase in theta coherence in response to tone onset (**Figure 5, right center column, bottom row**). This could indicate the existence of multiple distinct theta oscillators, overlapping in frequency, but with only one involving coherence between the mPFC and BLA. If the power of the non-coherent theta drops during fear

expression, the coherent theta may become more obvious, as in an increased signal-to-noise ratio.

Keeping the same gamma sub-bands as defined based on their differential expression in the Acquisition stage, the mid-gamma (45-60 Hz) band is clearly elevated throughout the Recall spectrograms (**Figure 4, right center column**). Low gamma (30-45 Hz) showed no significant changes in response to the tone except for one spurious decrease in mPFC-BLA coherence (**Figure 5, right center column, bottom row**). Mid-gamma, on the other hand, was significantly increased in mPFC power for up to 4 out of 5 rats, in BLA power for 2 of 5, and in coherence for 2 of 5 rats (**Figure 5, right center column**). High gamma (60-100 Hz) power in the mPFC was also significantly increased in response to tones for up to 3 out of 5 rats, while only spurious decreases appeared in BLA power or mPFC-BLA coherence (**Figure 5, right center column**). Notably, high gamma power in mPFC decreases for several seconds after tone offset in the Recall phase – the opposite pattern from Acquisition (**Figure 4, right center column, top row**).

3.3.4. Extinction

Finally, by the end of Extinction training, both regions had lost tone-responsivity in the low frequency domain (**Figure 4, right column**). Notably, there was an overall decrease in the power of the delta, theta, and beta bands, and an increase in mid- and high gamma frequency oscillations, that appeared to distinguish the Extinction trials from those of Habituation. However, since these changes were visible over the entire 90s trial period, there were no significant differences observed in the before vs. during tone

comparison, except for two spurious changes detected in one rat each (**Figure 5, right column**).

3.4. Neural correlates of behavior

In order to more precisely define which neural signals correlate specifically with fear expression as opposed to other processes that may be involved in fear learning and extinction memory, we took a detailed look at the continuous LFP recordings from the first extinction session during fear recall. This recording session was chosen because of the dramatic shifts in behavior from barpressing, to freezing in fear, and back to bar pressing again, that varied in timing amongst the five rats that met behavioral criteria. Rather than looking exclusively at feared tone responses, we calculated the correlation of % freezing in 6s bins with both regions' spectrograms and their mutual coherogram. In this way, we could generate a "spectral correlation" for each rat, and then determine which frequencies of which measures were positively or negatively correlated with fear expression. Bonferroni corrections were made for multiple comparisons: 3 neural measures * # of frequency bins. The group data for each measure is illustrated in **Figure 6,** which shows the number of rats with significant ($p < 0.05$) positive (blue) or negative (red) correlations of each frequency bin to % freezing, overlaid with the average correlation coefficient (R) for all 5 control rats.

For mPFC power, the delta frequency band (1-3 Hz) showed significant positive correlations with freezing in 3 out of the 5 control rats. In contrast, theta frequency (8-11

Hz) power was negatively correlated with freezing in all 5 control rats, with some expressing broader ranges. Gamma power in mPFC was also negatively correlated with freezing, in both low (30 - 45 Hz, up to 3 of 5 rats) and high (65 - 100 Hz, all 5 rats) frequency ranges, but not the mid gamma range (50 - 60 Hz), in which one rat showed a positive correlation with freezing.

The pattern of freezing correlations with BLA power was generally similar to that observed in the mPFC, with 4 of 5 rats showing a negative correlation with theta (7 - 9 Hz) power, and all 5 showing negative correlations with narrow portions of the low (40 - 45 Hz) and high (70 - 75 Hz) gamma frequency ranges. At least 2 rats maintained these negative correlations over the broader frequency ranges reported above for mPFC power correlations.

Coherence, however, showed a different pattern, with fewer rats showing any significant correlations with freezing. Up to 3 of the 5 control rats showed positive correlations with theta (9 - 11 Hz) coherence – in contrast to the negative correlations between freezing and either region's power. In the mid gamma frequency range (50 - 55 Hz) coherence was positively correlated with freezing behavior for 2 of 5 rats. Finally, up to 2 of 5 rats showed negative correlations between freezing and high gamma (85 - 100 Hz) coherence.

3.5. Cross-frequency coupling

Having established that the occurrence of low and high frequency oscillations in LFPs correlate with freezing behavior during fear recall, we next explored the possibility of functional interactions between these frequency bands. As phase-amplitude coupling had recently been detected in the mPFC during other tasks, we chose to examine whether the phase of the low frequency delta oscillation was modulating the amplitude of the gamma frequency oscillations during fear learning. The modulation indices (KL-MI) were calculated and converted into z-scores as described in Methods (Section 2.9). Significance at $p < 0.05$ was determined separately for each rat after applying Bonferroni correction for multiple comparisons (number of phase-amplitude frequency pairs tested). The resultant cross-frequency-coupling plots, referred to as comodulograms, for LFPs captured before, during and after CS presentation are illustrated in **Figure 7**.

As illustrated, the 12 comodulograms depict the change in cross-frequency coupling among pairs of frequencies across the four stages of fear learning and extinction and before, during, and after CS presentation within each trial. The color scale reflects the average z-score across all five rats for each pair of frequencies and the outlines depict smoothed estimates of the number of rats showing significant coupling within specific areas. The white line is an isocontour indicating at least two rats showed significant coupling within the region enclosed by a white outline. Likewise, the black outline is an isocontour indicating at least four rats showing significant coupling within the region enclosed by the black outline.

Notably, there is a baseline pattern of cross-frequency modulation that is consistent across all panels of the comodulogram. This includes at least two separate regions of significance for at least two rats: delta modulation of mid gamma and theta modulation of high gamma. In periods associated with high fear expression (Acquisition and Recall), however, the strength of the comodulation, as reflected in the average z-scores as well as number of rats showing significant coupling, was greatly enhanced. Specifically, regions of the comodulograms were identified for which four or more of the five rats showed significant cross-frequency coupling, both in an area predicted based on the observed power changes (delta modulation of mid gamma) and also in an unexpected region (low theta coupling with high gamma). The former is present during CS presentation in acquisition as well as both during and after CS presentation in recall, while the latter is most pronounced during CS presentation during acquisition but is also present before and after CS presentation in acquisition tones and during and after CS presentation in recall.

Figure 8 reflects the average phase of maximal gamma power within each delta/theta oscillation, using only the frequency pairs and rats that were found significant. Thus, every black pixel in these comodulograms reflects a frequency pair that was not significantly coupled for any of the five control rats. The most striking feature of this figure—aside from the consistency of the phase relationships throughout time, stages of fear learning and extinction, and even across rats—is the extremely sharp separation of the previously mentioned delta modulation of mid gamma from high gamma's modulation by delta/theta.

4. Discussion

Using multielectrode recording of local field potentials (LFPs) in the medial prefrontal cortex (mPFC) and basolateral complex of the amygdala (BLA) of freely moving rats undergoing Pavlovian fear conditioning, we investigated functional interactions between these two regions during fear learning and subsequent extinction. We report that LFPs in these two regions displayed dramatically different patterns of oscillatory activity across the stages of fear learning and extinction. Furthermore, we discovered interactions between low and high frequency oscillations that appear to be modulated differentially with respect to specific components of the fear learning paradigm, and deserve further exploration. Questions remain as to which oscillations and interactions are involved in the behavioral expression of fear, fear as an emotional experience, the cognitive representation of fear, and/or the learning processes of encoding, consolidation, retrieval, reconsolidation, extinction, and extinction retrieval.

4.1. Low Frequency (<30 Hz) Oscillations

Beginning with the lowest frequencies, both regions displayed significantly increased power, and coherence between regions, in a sharply tuned band in the delta frequency range (2-5 Hz) during successful fear acquisition and recall, as compared to baseline (before habituation tones). Power in mPFC delta during fear recall and early extinction was positively correlated with freezing behavior in the majority of rats.

However, the significant increase in mPFC delta power in response to the onset of feared tones during Recall was equally consistent – both reaching significance in 3 of 5 rats.

Interestingly, this same tone-triggered increase in mPFC delta power was even more consistent (4 out of 5 rats) during Acquisition, even though the behavior at that time was less specific to tones. That is, the rats were already freezing before the next tone came on, yet the delta band still increased in power, and slightly in frequency, at tone onset. This suggests that the delta oscillation is not merely a correlate of the behavioral expression of fear by freezing, and it may play a critical role in encoding the association between tone and shock, and in consolidating the fear memory for later retrieval. It is, in fact, a better substrate for linking the CS and US than the firing activity of individual neurons, as those tend to fire most strongly at tone onset but do not continue throughout the 30s tone to coincide with the footshock, whereas the delta oscillation absolutely does.

Its return during fear recall, then, may imply a separate but related role of delta in fear memory retrieval, which returns the memory to a labile state, ready for reconsolidation (if the CS-US pairing is reinforced) or novel extinction learning if not. The continuation of increased delta power and coherence after tone offset during fear recall supports the plausibility of this band playing a functional role in early extinction learning, perhaps facilitating the processing of an error signal received when the expected shock is not delivered. Its absence in late extinction, however, suggests that delta is likely not involved in the retrieval of an established extinction memory.

Similarly, low theta frequency (4-6 Hz) power and coherence between BLA, mPFC, and ventral hippocampus have been observed in freely moving mice expressing

fear memory, and this pattern diminishes upon extinction (Lesting et al., 2011). This low theta band, while nominally separated from the sharply tuned high delta oscillation (2-5 Hz) we found here, acts so similarly that it is very likely a result of the same neural substrate, simply expressed at a slightly different frequency range in mice than in rats. Interestingly, the delta association with state and trait anxiety, reward, and motivational salience in humans suggest that rats may be the more closely related species for translational research (Schutter and Knyazev, 2012).

Moreover, at least one other group has observed a 2 to 4 Hz delta oscillation during trace fear conditioning and expression in mice (Steenland et al., 2010). The discrepancy between studies may also relate to poorly chosen filtering thresholds or experimental design features that limit access to delta frequency signals, such as restricting data analysis to the very short windows of time between ~1 Hz tone pips (*e.g.*, Headley and Weinberger, 2013; Likhtik et al., 2014). Indeed, our delta band observation is a better fit with the intrinsic resonance frequencies measured in rat BLA projection cells, and with the spontaneous *in vitro* pattern of rhythmic inhibition (Ryan et al., 2012).

To further distinguish the delta and theta bands, in our experiment, there were clearly separable changes above and below ~6 Hz, making that a more appropriate dividing line than the usual 4 Hz. Specifically, during fear recall, a significant decrease in higher theta power (8-12 Hz) was detected in both regions. Power in this band was negatively correlated with freezing in all 5 rats in mPFC and 4 of 5 in BLA. This contrasts with the minimal level of significantly decreased theta power in mPFC and BLA upon tone onset (1 and 2 rats, respectively), suggesting that decreased activity in

this band more clearly reflects only the behavioral expression of fear by freezing, and likely does not play an important role in the association of CS and US or in the cue-triggered retrieval of the fear memory.

However, an overlapping theta frequency band (6-9 Hz) actually increased in coherence between the two regions of interest and was positively correlated with freezing behavior in 3 rats and significantly increased at tone onset for 2 rats during fear recall. This may reflect the existence of multiple overlapping mechanisms and functions for the theta band – one associated with locomotion, which is suppressed during freezing, allowing an increase in "signal-to-noise" ratio for a fear-related theta oscillation that is coherent between mPFC and BLA. There was no such increase in theta coherence at tone onset for the acquisition trials, suggesting an exclusive role in the retrieval or cognitive representation of the CS-US contingency, as opposed to consolidation or general expression of fear, which would have been equally if not more prevalent during Acquisition.

A novel increase in low beta band (13-17 Hz) power was found in the mPFC post-shock in the acquisition phase and at no other time throughout the experiment. In human EEG studies, beta oscillations have previously been associated with anger and aggression (Rusalova and Kostyunina, 2004), which are likely initial reactions to the painful footshock. However, this anthropomorphic speculation will need to be pursued more specifically in follow-up studies, perhaps by examining neural activity in response to other painful or non-painful aversive stimuli, as compared to socially aggressive behavior.

As a general rule, low frequency power was weaker in the BLA than in the mPFC, with less dynamic range leading to smaller effects observed in response to fear. This finding was somewhat surprising, considering that we had initially predicted delta oscillations due to the *in vitro* firing properties of BLA neurons (Ryan et al., 2012), but we believe it relates to the anatomical arrangement of neurons in the BLA – or more accurately, the lack of arrangement in layers of projection neurons all pointing their electrical dipoles in the same direction. That laminar construction of the cortex and hippocampus allow for large extracellular potentials to summate at both slow and fast timescales. In the BLA, however, only the electrical currents generated very close to the electrode, such as in a small cluster of surrounding neurons that happen to point toward or away from the electrode, will be detected. Since faster oscillations tend to represent more local processing, while slower oscillations allow (and perhaps require) the recruitment of larger populations of similarly oriented neurons, as described in **Section 1.2.3**, we suspect that electrodes in the BLA are biased against the detection of low frequency oscillations.

4.2. Gamma (30-100 Hz) Oscillations

Gamma activity that was significantly modulated over the course of the experiment could be functionally divided into three distinct bands: low (30-45 Hz), mid (45-60 Hz), and high (60-90 Hz) gamma. Throughout fear acquisition, the mid-gamma range was significantly elevated over baseline in terms of mPFC power, BLA power, and coherence between the two regions. After the shock, however, there were dramatic

increases in high gamma power for the mPFC and in low gamma power for the BLA. In contrast, after the expected shock is not delivered during fear recall / early extinction, high gamma power in the mPFC decreases for several seconds following tone offset, while there is no change from baseline in BLA low gamma power. This differential change in mPFC high gamma power, increasing after CS-US pairings and decreasing after un-reinforced CS presentations, may reflect distinct, opposing mechanisms for learning "to fear" during acquisition and "not to fear" during extinction. Further experiments, possibly using a partial reinforcement paradigm, will be needed to investigate this phenomenon in more detail.

These differential gamma frequency preferences of the two regions studied could reflect communication and phase-locking with other relevant brain regions involved in the response to a shock. For example, the BLA may be using the low gamma band to communicate with the rhinal cortex (Bauer et al., 2007) or striatum (Popescu et al., 2009), while the mPFC uses high gamma to communicate with auditory cortex (Headley and Weinberger, 2013). This is one of the most powerful aspects of neural oscillations: the same population of cells may express more than one bit of information at a time through the use of simultaneously active oscillatory patterns at different frequencies, tuned according to the resonant properties of the intended signal recipients. As described in **Section 1.3**, each cell automatically amplifies those synaptic inputs that arrive within the receptive phase of their own ongoing oscillations and ignores other inputs, effectively filtering out irrelevant information.

When examined during fear recall and early extinction, power in each region at both low and high gamma frequencies were negatively correlated with freezing behavior, while mid-gamma was conspicuously uncorrelated. Similar to the observation at theta frequency, coherence between the two regions in this mid-gamma range was actually positively correlated with freezing behavior in two of five rats, despite overlapping in some frequencies that showed negative correlations between power in each region and freezing. Even more noticeably distinct is the pattern of tone-triggered changes in power, representative of the retrieval and possible reconsolidation or extinction of the learned fear, as compared to the spectral correlates of freezing as a behavioral expression of fear.

High gamma power in the mPFC, for example, significantly increases in response to the feared tone in up to 3 of the 5 rats (~65 Hz), but is negatively correlated with freezing for 4 of 5 rats at the same frequency. If we presume freezing to be an accurate measure of the emotional experience of fear, this evidence would suggest that gamma must not be directly involved in the emotion, but perhaps more tightly linked with the cognitive processes of cue processing and memory retrieval. Alternatively, if gamma is linked to the emotional experience of fear, the negative correlation with freezing could be explained by an inverted-U-shaped curve, wherein the lack of fear is expressed by no freezing, some fear is expressed by freezing, but the highest levels of fear are expressed through active escape measures that preclude freezing, and high gamma may only correlate with this highest fear condition, when there is a negative correlation between freezing and fear. While emotional and cognitive experiences are inherently difficult to observe in animals, these possible explanations may be easier to parse out using an active

avoidance paradigm and/or the addition of autonomic telemetry and recording of ultrasonic vocalizations to detect other correlates of fear.

The human amygdala, recorded by intracranial electrodes in epilepsy patients, rapidly reacts to fearful facial expressions with increased gamma power (Sato et al., 2011). Gamma power is also known to increase during fear behavior in both mPFC (Fitzgerald et al., 2013b) and the auditory cortex (Headley and Weinberger, 2013). However, the current study is, to the best of our knowledge, the first to demonstrate significant alterations in gamma activity in the amygdala in association with fear conditioning in rodents.

4.3. Cross-Frequency Coupling

The unique dynamics of each frequency band, however, do not give a complete picture of the interactions between frequencies. Our analysis of Cross-Frequency Coupling (CFC) in the mPFC demonstrates the presence of at least two distinct pairs of frequency bands for which the amplitude of the higher frequency oscillation is significantly modulated by the phase of the lower frequency oscillation. Furthermore, each pair has a consistent phase preference that is remarkably stable across time, stages of fear learning and extinction, and even conserved across animals, while the magnitude of the modulation varies greatly according to those same criteria. First, in the bands predicted based on the most prominent peaks of the power spectrum, the mid-gamma

oscillation strongly prefers the trough of the mPFC delta oscillation during anticipatory fear (cue presentation during late acquisition and during recall / early extinction).

Second, a wider range of delta / theta frequencies also modulates mid to high gamma oscillations with a consistent pattern of phase preferences. Alternatively, this could be interpreted either as delta/theta phase modulation of different frequency gamma oscillations' amplitudes, or as delta/theta phase modulation of gamma frequency. Since we approached the data looking for phase-amplitude coupling, this alternate hypothesis of phase-frequency coupling cannot be confirmed or rejected without undertaking a new analysis. Given the phase relationships apparent in the current results, if phase-frequency coupling was the dominant form of modulation by a narrowly filtered low-theta (6-8 Hz) oscillation, we would expect a wide gamma filtered signal to have power concentrated around 100 Hz just before the peak, gradually slowing to 70 Hz on the falling phase, and bottoming out around 50 Hz just before the trough of the low theta oscillation. Near the trough and rising phase of low theta, gamma power may be lower, or the frequency may simply be less consistent in this phase.

Complicating the situation further, if we examined gamma frequency modulation by a narrowly filtered high-theta (8-10 Hz) oscillation instead, the expected pattern would be remarkably similar, just shifted a tiny bit later in the phase. Since neither of these theta sub-bands was represented by a prominent peak in the power spectra, and since high theta actually decreased significantly during fear expression, it is difficult to understand how they would be in a position to consistently modulate the same frequencies of gamma in such similar patterns with respect to phase, even when they would almost certainly

overlap and conflict with each other in time. This introduces some suspicion that the theta-gamma coupling we observed here may relate to some kind of artifact produced by the repeated filtering of non-sinusoidal LFPs into narrow frequency bands. Luckily, a novel analytic method has recently been proposed to virtually eliminate filtering from the analysis of phase-amplitude coupling (Dvorak and Fenton, 2014). I look forward to applying that data-driven approach.

Returning to the predicted and verified delta phase modulation of mid-gamma amplitude, the mechanisms and functions seem easier to grasp. The increased power in each band, and their cross-frequency co-modulation, continues from beginning to end of the tone during acquisition, and well beyond the end of the tone during recall. Thus, this complex oscillatory pattern is a more likely mediator of the synaptic plasticity necessary to associate the CS and US, and to suppress that association during extinction learning, as compared to the short lived firing rate changes of individual neurons in response to stimulus onset. We would predict these oscillatory interactions to perform this function equally well in a trace conditioning paradigm, wherein the CS and US do not coincide in time at all, but the shock input would still coincide with the delta oscillation. Indeed, very similar activity has recently been observed for theta phase modulation of gamma oscillations in the mPFC during the trace interval in trace eye-blink conditioning (Shearkhani and Takehara-Nishiuchi, 2013). Moreover, human studies have also observed emotionally-related delta phase modulation of beta or gamma amplitude, which is proposed as an integral substrate of cortical-subcortical interactions (Schutter and Knyazev, 2012).

4.4. Conclusions and Future Directions

In summary, feared tones triggered increases in both the delta and mid-gamma bands in mPFC power, BLA power, and coherence between the two regions. These changes seem linked to the cognitive/emotional representation of fear and/or the memory encoding and retrieval processes, whereas the expression of fear by freezing is strongly correlated with decreases in theta, low-gamma, and high-gamma power in both regions. Furthermore, the phase of the mPFC delta oscillation during feared tones was found to modulate the amplitude of the mPFC mid-gamma oscillation, which was in turn coherent with mid-gamma oscillations in the BLA. Thus, we infer that these multi-dimensional interactions across regions and frequencies serve to coordinate information transfer across multiple spatiotemporal scales, allowing dynamic and flexible associations between stimuli and their affective/motivational salience.

While this study has been based primarily on observation and correlation, our future studies will be focused on demonstrating the causal roles of particular cell types, neuromodulators, and afferent input patterns in producing both the observed oscillations and their corresponding behavioral representations. Furthermore, the analytical techniques developed here will be adapted to the analysis of clinical neurophysiology data and hopefully used to directly improve the treatment of neuropsychiatric disease.

5. References

Adhikari A, Topiwala MA, Gordon JA (2010) Synchronized activity between the ventral hippocampus and the medial prefrontal cortex during anxiety. Neuron 65:257–269.

Adhikari A, Topiwala MA, Gordon JA (2011) Single units in the medial prefrontal cortex with anxiety-related firing patterns are preferentially influenced by ventral hippocampal activity. Neuron 71:898–910.

Albers C, Schmiedt JT, Pawelzik KR (2013) Theta-specific susceptibility in a model of adaptive synaptic plasticity. Front Comput Neurosci 7:170.

Alcaro A, Panksepp J (2011) The SEEKING mind: primal neuro-affective substrates for appetitive incentive states and their pathological dynamics in addictions and depression. Neurosci Biobehav Rev 35:1805–1820.

Başar E (2013) Brain oscillations in neuropsychiatric disease. Dialogues Clin Neurosci 15:291–300.

Bauer EP, Paz R, Paré D (2007) Gamma oscillations coordinate amygdalo-rhinal interactions during learning. J Neurosci 27:9369–9379.

Benes FM (2010) Amygdalocortical circuitry in schizophrenia: from circuits to molecules. Neuropsychopharmacology 35:239–257.

Berens P (2009) CircStat: a MATLAB toolbox for circular statistics. J Stat Softw 31.

Bienvenu TCM, Busti D, Magill PJ, Ferraguti F, Capogna M (2012) Cell-type-specific recruitment of amygdala interneurons to hippocampal theta rhythm and noxious stimuli in vivo. Neuron 74:1059–1074.

Bokil H, Andrews P, Kulkarni JE, Mehta S, Mitra PP (2010) Chronux: A platform for analyzing neural signals. J Neurosci Methods 192:146–151.

Bokil H, Purpura K, Schoffelen J-M, Thomson D, Mitra P (2007) Comparing spectra and coherences for groups of unequal size. J Neurosci Methods 159:337–345.

Buzsáki G, Anastassiou CA, Koch C (2012) The origin of extracellular fields and currents--EEG, ECoG, LFP and spikes. Nat Rev Neurosci 13:407–420.

Buzsáki G, Draguhn A (2004) Neuronal oscillations in cortical networks. Science (80-) 304:1926–1929.

Buzsáki G, Wang X-J (2012) Mechanisms of gamma oscillations. Annu Rev Neurosci 35:203–225.

Buzsáki G, Watson BO (2012) Brain rhythms and neural syntax: implications for efficient coding of cognitive content and neuropsychiatric disease. Dialogues Clin Neurosci 14:345–367.

Canolty RT, Knight RT (2010) The functional role of cross-frequency coupling. Trends Cogn Sci 14:506–515.

Cardin JA, Carlén M, Meletis K, Knoblich U, Zhang F, Deisseroth K, Tsai L-H, Moore CI (2009) Driving fast-spiking cells induces gamma rhythm and controls sensory responses. Nature 459:663–667.

Colgin LL (2011) Oscillations and hippocampal-prefrontal synchrony. Curr Opin Neurobiol 21:467–474.

Colgin LL (2013) Mechanisms and functions of theta rhythms. Annu Rev Neurosci 36:295–312.

Courtin J, Bienvenu TCM, Einarsson EÖ, Herry C (2013a) Medial prefrontal cortex neuronal circuits in fear behavior. Neuroscience 240:219–242.

Courtin J, Chaudun F, Rozeske RR, Karalis N, Gonzalez-Campo C, Wurtz H, Abdi A, Baufreton J, Bienvenu TCM, Herry C (2014) Prefrontal parvalbumin interneurons shape neuronal activity to drive fear expression. Nature 505:92–96.

Courtin J, Karalis N, Gonzalez-Campo C, Wurtz H, Herry C (2013b) Persistence of amygdala gamma oscillations during extinction learning predicts spontaneous fear recovery. Neurobiol Learn Mem.

Dan Y, Poo M-M (2006) Spike timing-dependent plasticity: from synapse to perception. Physiol Rev 86:1033–1048.

Davis M, Rainnie DG, Cassell M (1994) Neurotransmission in the rat amygdala related to fear and anxiety. Trends Neurosci 17:208–214.

Delorme A, Makeig S (2004) EEGLAB: an open source toolbox for analysis of single-trial EEG dynamics including independent component analysis. J Neurosci Methods 134:9–21.

Dvorak D, Fenton AA (2014) Toward a proper estimation of phase-amplitude coupling in neural oscillations. J Neurosci Methods 225:42–56.

Fitzgerald PJ, Whittle N, Flynn SM, Graybeal C, Pinard CR, Gunduz-Cinar O, Kravitz A V, Singewald N, Holmes A (2013a) Prefrontal single-unit firing associated with deficient extinction in mice. Neurobiol Learn Mem.

Fitzgerald THB, Valentin A, Selway R, Richardson MP (2013b) Cross-frequency coupling within and between the human thalamus and neocortex. Front Hum Neurosci 7:84.

Fujisawa S, Buzsáki G (2011) A 4 Hz oscillation adaptively synchronizes prefrontal, VTA, and hippocampal activities. Neuron 72:153–165.

Garolera M, Coppola R, Muñoz KE, Elvevåg B, Carver FW, Weinberger DR, Goldberg TE (2007) Amygdala activation in affective priming: a magnetoencephalogram study. Neuroreport 18:1449–1453.

Hartwich K, Pollak T, Klausberger T (2009) Distinct firing patterns of identified basket and dendrite-targeting interneurons in the prefrontal cortex during hippocampal theta and local spindle oscillations. J Neurosci 29:9563–9574.

Headley DB, Paré D (2013) In sync: gamma oscillations and emotional memory. Front Behav Neurosci 7:170.

Headley DB, Weinberger NM (2011) Gamma-band activation predicts both associative memory and cortical plasticity. J Neurosci 31:12748–12758.

Headley DB, Weinberger NM (2013) Fear conditioning enhances γ oscillations and their entrainment of neurons representing the conditioned stimulus. J Neurosci 33:5705–5717.

Hentschke H, Perkins MG, Pearce R a, Banks MI (2007) Muscarinic blockade weakens interaction of gamma with theta rhythms in mouse hippocampus. Eur J Neurosci 26:1642–1656.

Herry C, Ferraguti F, Singewald N, Letzkus JJ, Ehrlich I, Lüthi A (2010) Neuronal circuits of fear extinction. Eur J Neurosci 31:599–612.

Huff ML, Miller RL, Deisseroth K, Moorman DE, LaLumiere RT (2013) Posttraining optogenetic manipulations of basolateral amygdala activity modulate consolidation of inhibitory avoidance memory in rats. Proc Natl Acad Sci U S A 110:3597–3602.

Hyman JM, Wyble BP, Goyal V, Rossi CA, Hasselmo ME (2003) Stimulation in hippocampal region CA1 in behaving rats yields long-term potentiation when delivered to the peak of theta and long-term depression when delivered to the trough. J Neurosci 23:11725–11731.

Insel TR, Landis SC (2013) Twenty-five years of progress: the view from NIMH and NINDS. Neuron 80:561–567.

Kamarajan C, Rangaswamy M, Manz N, Chorlian DB, Pandey AK, Roopesh BN, Porjesz B (2012) Topography, power, and current source density of θ oscillations during reward processing as markers for alcohol dependence. Hum Brain Mapp 33:1019–1039.

Klimesch W, Freunberger R, Sauseng P (2010) Oscillatory mechanisms of process binding in memory. Neurosci Biobehav Rev 34:1002–1014.

Knyazev GG (2007) Motivation, emotion, and their inhibitory control mirrored in brain oscillations. Neurosci Biobehav Rev 31:377–395.

Lesting J, Daldrup T, Narayanan V, Himpe C, Seidenbecher T, Pape H-C (2013) Directional theta coherence in prefrontal cortical to amygdalo-hippocampal pathways signals fear extinction. PLoS One 8:e77707.

Lesting J, Narayanan RT, Kluge C, Sangha S, Seidenbecher T, Pape H-C (2011) Patterns of Coupled Theta Activity in Amygdala-Hippocampal-Prefrontal Cortical Circuits during Fear Extinction. PLoS One 6:e21714.

Lewis DA, Curley AA, Glausier JR, Volk DW (2012) Cortical parvalbumin interneurons and cognitive dysfunction in schizophrenia. Trends Neurosci 35:57–67.

Li C, Dabrowska J, Hazra R, Rainnie DG (2011) Synergistic activation of dopamine D1 and TrkB receptors mediate gain control of synaptic plasticity in the basolateral amygdala. PLoS One 6:e26065.

Likhtik E, Stujenske JM, Topiwala MA, Harris AZ, Gordon JA (2014) Prefrontal entrainment of amygdala activity signals safety in learned fear and innate anxiety. Nat Neurosci 17:106–113.

Lipponen A, Woldemichael BT, Gurevicius K, Tanila H (2012) Artificial theta stimulation impairs encoding of contextual fear memory. PLoS One 7:e48506.

Lisman J (2012) Excitation, inhibition, local oscillations, or large-scale loops: what causes the symptoms of schizophrenia? Curr Opin Neurobiol 22:537–544.

Lisman JE, Jensen O (2013) The θ-γ neural code. Neuron 77:1002–1016.

López-Azcárate J, Nicolás MJ, Cordon I, Alegre M, Valencia M, Artieda J (2013) Delta-mediated cross-frequency coupling organizes oscillatory activity across the rat cortico-basal ganglia network. Front Neural Circuits 7:155.

Marek R, Strobel C, Bredy TW, Sah P (2013) The amygdala and medial prefrontal cortex: partners in the fear circuit. J Physiol 591:2381–2391.

Maroun M (2013) Medial prefrontal cortex: multiple roles in fear and extinction. Neuroscientist 19:370–383.

Mascagni F, Muly EC, Rainnie DG, McDonald AJ (2009) Immunohistochemical characterization of parvalbumin-containing interneurons in the monkey basolateral amygdala. Neuroscience 158:1541–1550.

McDonald AJ, Mascagni F, Mania I, Rainnie DG (2005) Evidence for a perisomatic innervation of parvalbumin-containing interneurons by individual pyramidal cells in the basolateral amygdala. Brain Res 1035:32–40.

McNaughton N, Swart C, Neo P, Bates V, Glue P (2013) Anti-anxiety drugs reduce conflict-specific "theta"--a possible human anxiety-specific biomarker. J Affect Disord 148:104–111.

Milad MR, Quirk GJ (2012) Fear extinction as a model for translational neuroscience: ten years of progress. Annu Rev Psychol 63:129–151.

Miskovic V, Moscovitch DA, Santesso DL, McCabe RE, Antony MM, Schmidt LA (2011) Changes in EEG cross-frequency coupling during cognitive behavioral therapy for social anxiety disorder. Psychol Sci 22:507–516.

Muly EC, Senyuz M, Khan ZU, Guo J-D, Hazra R, Rainnie DG (2009) Distribution of D1 and D5 dopamine receptors in the primate and rat basolateral amygdala. Brain Struct Funct 213:375–393.

Narayanan RT, Seidenbecher T, Kluge C, Bergado J, Stork O, Pape H-C (2007) Dissociated theta phase synchronization in amygdalo- hippocampal circuits during various stages of fear memory. Eur J Neurosci 25:1823–1831.

Nishida M, Pearsall J, Buckner RL, Walker MP (2009) REM sleep, prefrontal theta, and the consolidation of human emotional memory. Cereb Cortex 19:1158–1166.

Orsini CA, Maren S (2012) Neural and cellular mechanisms of fear and extinction memory formation. Neurosci Biobehav Rev 36:1773–1802.

Oya H, Kawasaki H, Howard MA, Adolphs R (2002) Electrophysiological responses in the human amygdala discriminate emotion categories of complex visual stimuli. J Neurosci 22:9502–9512.

Pape H-C, Narayanan RT, Smid J, Stork O, Seidenbecher T (2005) Theta activity in neurons and networks of the amygdala related to long-term fear memory. Hippocampus 15:874–880.

Pape H-C, Paré D (2010) Plastic synaptic networks of the amygdala for the acquisition, expression, and extinction of conditioned fear. Physiol Rev 90:419–463.

Parsons RG, Ressler KJ (2013) Implications of memory modulation for post-traumatic stress and fear disorders. Nat Neurosci 16:146–153.

Popa D, Duvarci S, Popescu AT, Léna C, Paré D (2010) Coherent amygdalocortical theta promotes fear memory consolidation during paradoxical sleep. Proc Natl Acad Sci U S A 107:6516–6519.

Popescu AT, Popa D, Paré D (2009) Coherent gamma oscillations couple the amygdala and striatum during learning. Nat Neurosci 12:801–807.

Popov T, Steffen A, Weisz N, Miller GA, Rockstroh B (2012) Cross-frequency dynamics of neuromagnetic oscillatory activity: Two mechanisms of emotion regulation. Psychophysiology 49:1545–1557.

Quirk GJ, Russo GK, Barron JL, Lebron K (2000) The role of ventromedial prefrontal cortex in the recovery of extinguished fear. J Neurosci 20:6225–6231.

Rainnie DG (1999) Serotonergic modulation of neurotransmission in the rat basolateral amygdala. J Neurophysiol 82:69–85.

Rainnie DG, Asprodini EK, Shinnick-Gallagher P (1991a) Excitatory transmission in the basolateral amygdala. J Neurophysiol 66:986–998.

Rainnie DG, Asprodini EK, Shinnick-Gallagher P (1991b) Inhibitory transmission in the basolateral amygdala. J Neurophysiol 66:999–1009.

Randall FE, Whittington MA, Cunningham MO (2011) Fast oscillatory activity induced by kainate receptor activation in the rat basolateral amygdala in vitro. Eur J Neurosci 33:914–922.

Reeves WC, Strine TW, Pratt LA, Thompson W, Ahluwalia I, Dhingra SS, McKnight-Eily LR, Harrison L, D'Angelo D V, Williams L, Morrow B, Gould D, Safran MA (2011) Mental illness surveillance among adults in the United States. MMWR Surveill Summ 60 Suppl 3:1–29.

Rusalova MN, Kostyunina MB (2004) Spectral correlation studies of emotional states in humans. Neurosci Behav Physiol 34:803–808.

Ryan SJ, Ehrlich DE, Jasnow AM, Daftary S, Madsen TE, Rainnie DG (2012) Spike-timing precision and neuronal synchrony are enhanced by an interaction between synaptic inhibition and membrane oscillations in the amygdala. PLoS One 7:e35320.

Sangha S, Narayanan RT, Bergado-Acosta JR, Stork O, Seidenbecher T, Pape H-C (2009) Deficiency of the 65 kDa isoform of glutamic acid decarboxylase impairs extinction of cued but not contextual fear memory. J Neurosci 29:15713–15720.

Sato W, Kochiyama T, Uono S, Matsuda K, Usui K, Inoue Y, Toichi M (2011) Rapid amygdala gamma oscillations in response to fearful facial expressions. Neuropsychologia 49:612–617.

Schutter DJLG, Knyazev GG (2012) Cross-frequency coupling of brain oscillations in studying motivation and emotion. Motiv Emot 36:46–54.

Seidenbecher T, Laxmi TR, Stork O, Pape H-C (2003) Amygdalar and hippocampal theta rhythm synchronization during fear memory retrieval. Science (80-) 301:846–850.

Senn V, Wolff SB, Herry C, Grenier F, Ehrlich I, Gründemann J, Fadok JP, Müller C, Letzkus JJ, Lüthi A (2014) Long-Range Connectivity Defines Behavioral Specificity of Amygdala Neurons. Neuron 81:428–437.

Shearkhani O, Takehara-Nishiuchi K (2013) Coupling of prefrontal gamma amplitude and theta phase is strengthened in trace eyeblink conditioning. Neurobiol Learn Mem 100:117–126.

Sinfield JL, Collins DR (2006) Induction of synchronous oscillatory activity in the rat lateral amygdala in vitro is dependent on gap junction activity. Eur J Neurosci 24:3091–3095.

Sohal VS (2012) Insights into cortical oscillations arising from optogenetic studies. Biol Psychiatry 71:1039–1045.

Sohal VS, Zhang F, Yizhar O, Deisseroth K (2009) Parvalbumin neurons and gamma rhythms enhance cortical circuit performance. Nature 459:698–702.

Steenland HW, Wu V, Fukushima H, Kida S, Zhuo M (2010) CaMKIV over-expression boosts cortical 4-7 Hz oscillations during learning and 1-4 Hz delta oscillations during sleep. Mol Brain 3:16.

Steriade M, Nuñez A, Amzica F (1993) A novel slow (< 1 Hz) oscillation of neocortical neurons in vivo: depolarizing and hyperpolarizing components. J Neurosci 13:3252–3265.

Stevenson CW, Halliday DM, Marsden CA, Mason R (2007) Systemic administration of the benzodiazepine receptor partial inverse agonist FG-7142 disrupts corticolimbic network interactions. Synapse 61:646–663.

Tort ABL, Komorowski R, Eichenbaum H, Kopell N (2010) Measuring phase-amplitude coupling between neuronal oscillations of different frequencies. J Neurophysiol 104:1195–1210.

Uhlhaas PJ, Singer W (2012) Neuronal dynamics and neuropsychiatric disorders: toward a translational paradigm for dysfunctional large-scale networks. Neuron 75:963–980.

VanElzakker MB, Kathryn Dahlgren M, Caroline Davis F, Dubois S, Shin LM (2013) From Pavlov to PTSD: The extinction of conditioned fear in rodents, humans, and anxiety disorders. Neurobiol Learn Mem.

Wang X-J (2010) Neurophysiological and computational principles of cortical rhythms in cognition. Physiol Rev 90:1195–1268.

Williams MA, Sachdev PS (2010) Magnetoencephalography in neuropsychiatry: ready for application? Curr Opin Psychiatry 23:273–277.

6. Figures and Legends

Figure 1. Experimental protocol, histology, and fear behavior in response to each tone.

(A) This timeline of the experiment highlights, with a dashed box, the recording sessions with tone presentations, as all the data analyzed in C and all subsequent figures come from these 3 sessions. (B) Representative mapping of histologically verified electrode placements (circles) targeting mPFC (top row) and BLA (bottom row). Approximate anterior/posterior coordinates of each slice are given relative to bregma (Paxinos and Watson, 1997). (C) Two complementary measures of fear behavior: Barpress Suppression Ratio (left Y axis, dark gray) and % Freezing (right Y axis, light gray), each averaged across rats (n=5) during tone presentations (X axis). Error bars represent SEM.

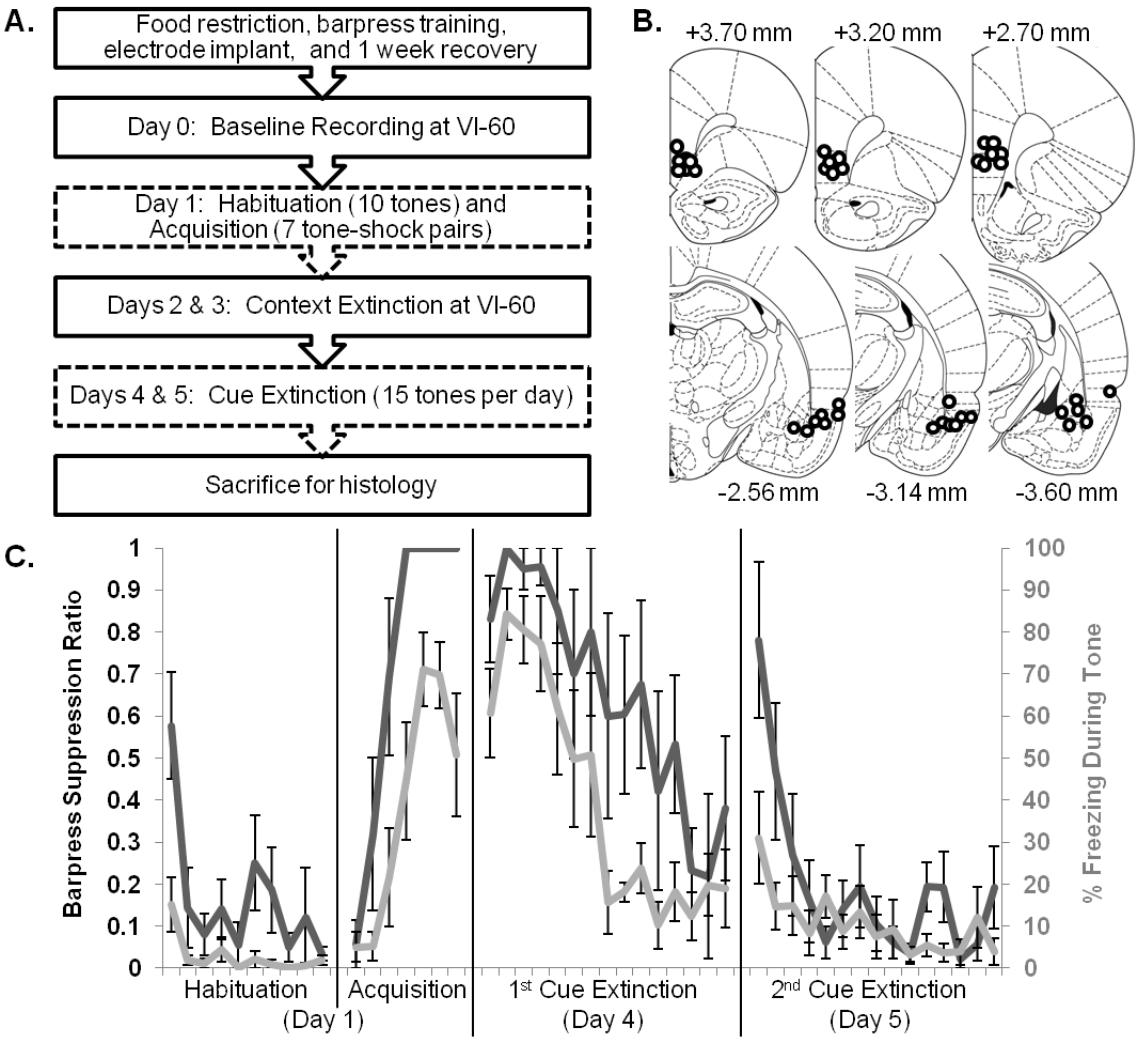
A.
Food restriction, barpress training, electrode implant, and 1 week recovery
Day 0: Baseline Recording at VI-60
Day 1: Habituation (10 tones) and Acquisition (7 tone-shock pairs)
Days 2 & 3: Context Extinction at VI-60
Days 4 & 5: Cue Extinction (15 tones per day)
Sacrifice for histology
B.
+3.70 mm
+3.20 mm
+2.70 mm
-2.56 mm
-3.14 mm
-3.60 mm
C.
Barpress Suppression Ratio
% Freezing During Tone
Habituation (Day 1)
Acquisition
1st Cue Extinction (Day 4)
2nd Cue Extinction (Day 5)

Figure 2. Cross-Frequency Coupling analysis flowchart.

The raw LFP signal is filtered into two distinct frequency bands: one in the delta/theta range, from which phase information is extracted, and one in the gamma range, from which the amplitude envelope is obtained. The phase of the low frequency signal is binned, and gamma amplitudes recorded during each phase bin are averaged. The distribution displayed in the bottom plot is an example of high CFC (from one mPFC electrode during Fear Recall), as the gamma amplitude increases at or shortly following each trough of the delta/theta oscillation.

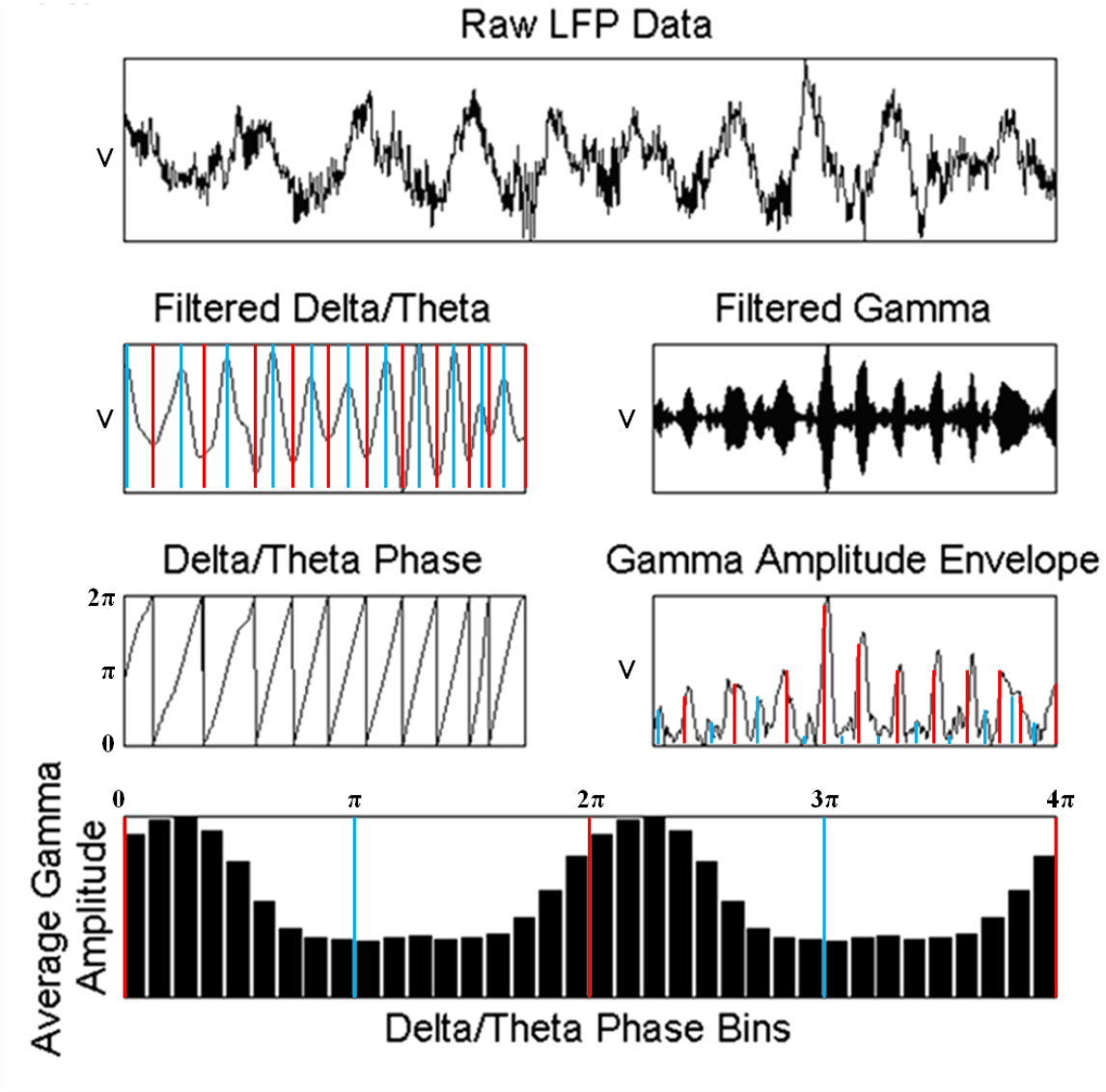
Raw LFP Data
V
Filtered Delta/Theta
V
Filtered Gamma
V
Delta/Theta Phase
2π
π
0
Gamma Amplitude Envelope
V
0
π
2π
3π
4π
Average Gamma Amplitude
Delta/Theta Phase Bins

Figure 3. Single trial example shows sharply tuned significant increase in delta power and significant decrease in theta power.

(A) Raw LFP signal recorded in the mPFC of one rat before (blue) and during (red) the first tone exposure in the first extinction session, *i.e.*, the first fear recall tone. Corresponding (B) autocorrelations and (C) power spectral densities. Error bars represent 95% confidence intervals. The inset is a spectrogram of the full trial including 30 seconds prior to and following tone delivery at t = 0 to 30 s. (D) Bokil Spectral Significance Test for difference between conditions (before vs. during tone). The black line is the value of the test statistic at each frequency; the dotted red lines are empirically determined significance thresholds based on the variance of the data at each frequency; the solid red lines represent a theoretical, frequency-independent significance threshold, and the blue bars denote frequency bands that change significantly in response to the tone.

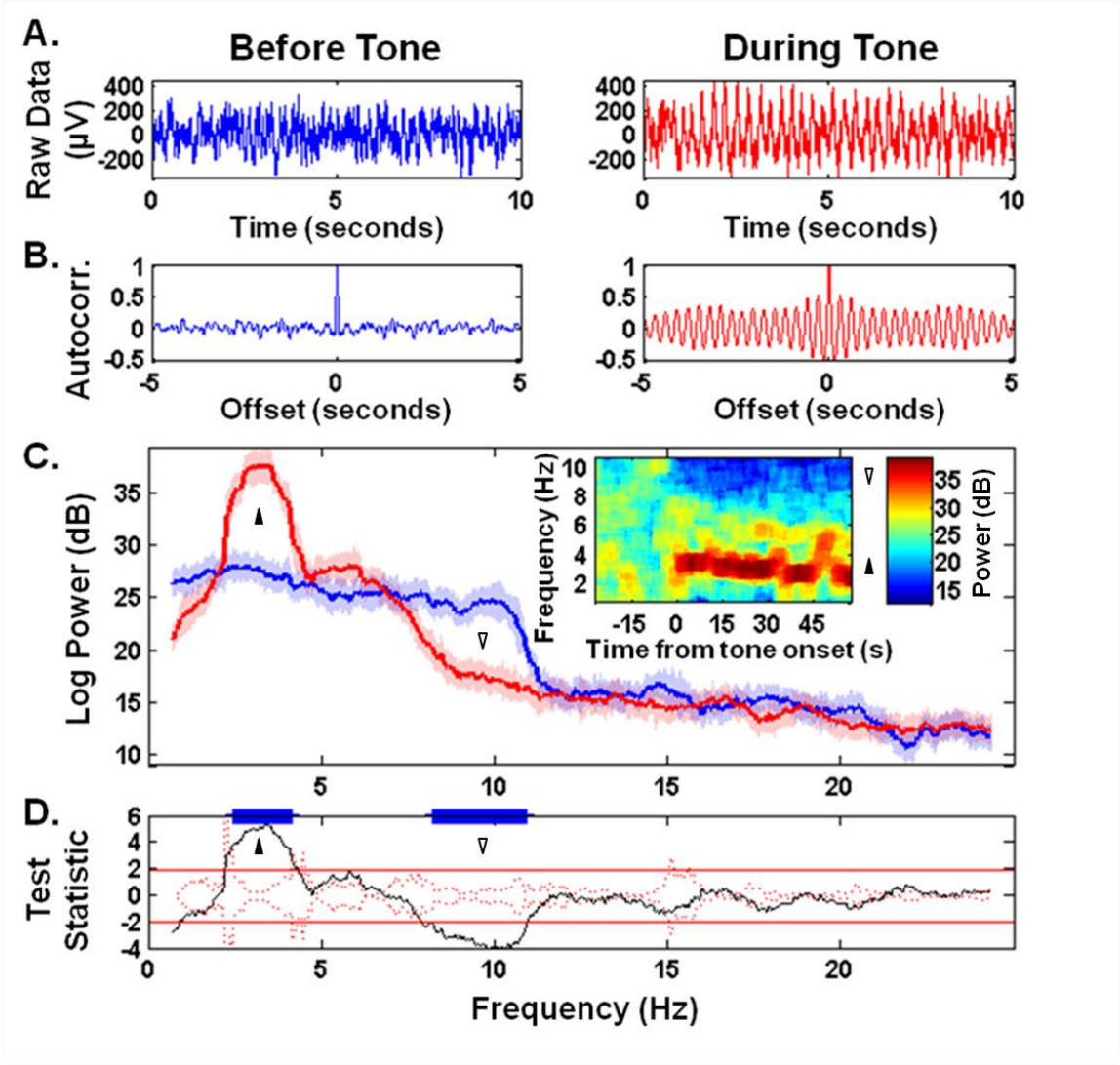
A.
Before Tone
During Tone
Raw Data (μV)
400
200
0
-200
0
5
10
Time (seconds)
B.
Autocorr.
1
0.5
0
-0.5
-5
0
5
Offset (seconds)
C.
Log Power (dB)
35
30
25
20
15
10
5
10
15
20
Frequency (Hz)
10
8
6
4
2
-15
0
15
30
45
Time from tone onset (s)
Power (dB)
35
30
25
20
15
D.
Test Statistic
6
4
2
0
-2
-4
0
5
10
15
20
Frequency (Hz)

Figure 4. Normalized spectrograms show increases and decreases in power over time and across phases of fear learning – coherent between mPFC and BLA.

The tone is presented from t = 0 to 30s in each plot. The prominent vertical line at 30s through all 3 rows of acquisition plots is an artifact of the footshock. All spectrograms and coherograms were calculated with 3 tapers over 1.33s windows (shifting by 10%), giving a spectral bandwidth (W) of ±1.5 Hz. (A) Average mPFC power change from baseline (before Habituation tones) across all 5 control rats. (B) Mean change in BLA power relative to same baseline. (C) Coherence measured between the same two electrodes used for the preceding spectrograms, averaged across rats without normalizing to baseline. The low end of the color scale is set to the theoretical confidence value for C > 0, such that all non-black pixels represent a significant level of coherence.

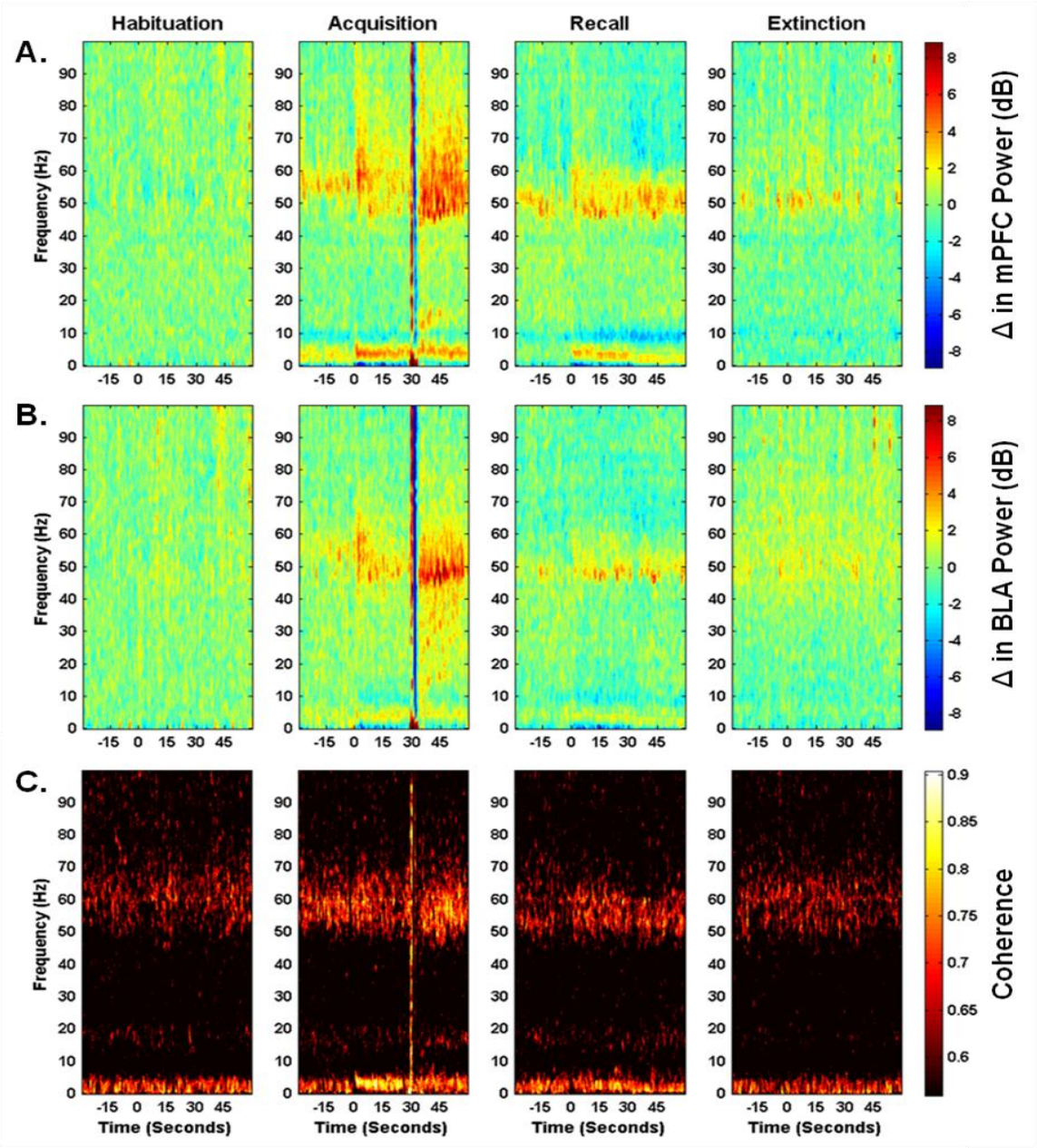
Habituation
Acquisition
Recall
Extinction
A.
B.
C.
Frequency (Hz)
Time (Seconds)
Δ in mPFC Power (dB)
Δ in BLA Power (dB)
Coherence

Figure 5. Significant spectral changes in response to fear conditioned tones.

Independently for each rat, the Bokil Spectral Comparison Test was applied to determine significant changes from before to during tones in each stage of fear learning and for all 3 spectral measures: mPFC power, BLA power, and mPFC-BLA coherence. The green lines represent the mean ± SEM Bokil test statistic across rats. Each plot also displays the number of rats that independently showed significant increases (blue) or decreases (red) in each spectral measure at each frequency bin.

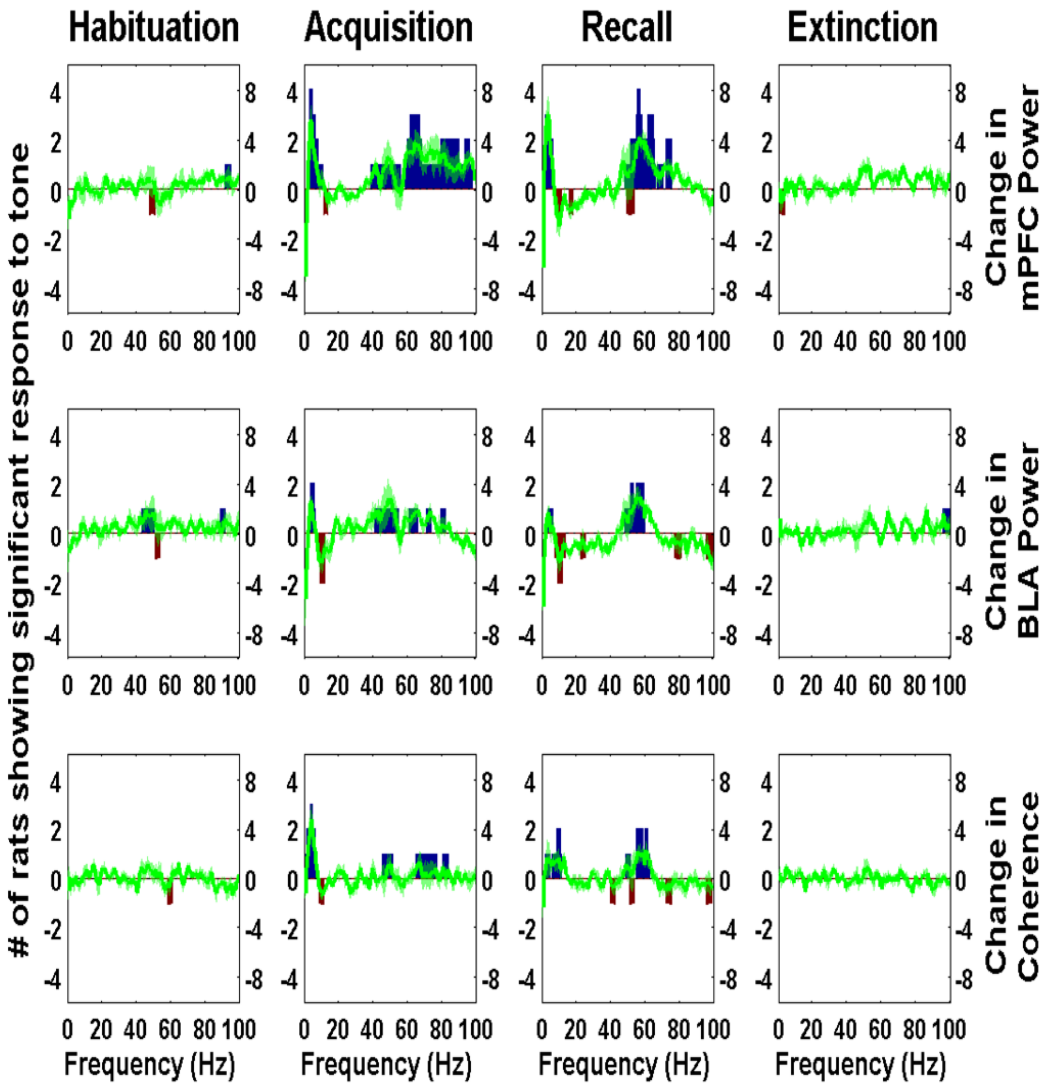
Habituation
Acquisition
Recall
Extinction
# of rats showing significant response to tone
Change in mPFC Power
Change in BLA Power
Change in Coherence
Frequency (Hz)
Frequency (Hz)
Frequency (Hz)
Frequency (Hz)

Figure 6. Spectral correlates of freezing behavior during fear recall.

Independently for each rat, the percent of time spent freezing in 6s bins throughout the first 45 minutes of the first extinction session was correlated with spectral estimates of mPFC power, BLA power, and mPFC-BLA coherence in the same 6s bins. The green lines represent the mean ± SEM correlation coefficient (R) at each frequency of all 5 rats who met behavioral criteria for both fear acquisition and extinction. Each plot also displays the number of rats that independently showed significant positive (blue) or negative (red) correlations between % freezing and each frequency bin.

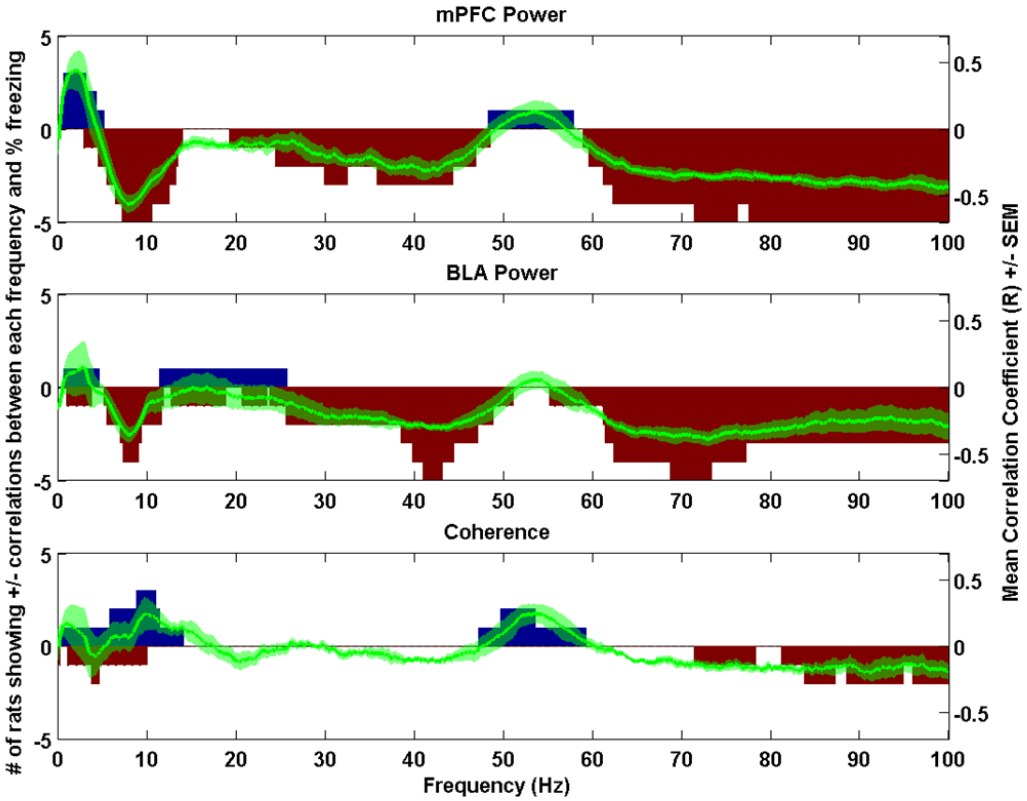
mPFC Power
BLA Power
Coherence
# of rats showing +/- correlations between each frequency and % freezing
Mean Correlation Coefficient (R) +/- SEM
Frequency (Hz)
5
0
-5
0.5
0
-0.5
0
10
20
30
40
50
60
70
80
90
100

Figure 7. Magnitude and significance of cross-frequency coupling.

Each comodulogram expresses the average Z-score across all 5 rats who met behavioral criteria for both fear acquisition & extinction, with each pixel corresponding to amplitude modulation of the frequency on the y-axis by the phase of the frequency on the x-axis. These are overlaid with iso-contours representing a smoothed outline around the region of significance for at least 2 of 5 rats (white) and for at least 4 of 5 rats (black). Each column corresponds to the stage of fear conditioning and extinction, while each row corresponds to ~*30s* segments before (A), during (B), and after (C) a single tone for each rat.

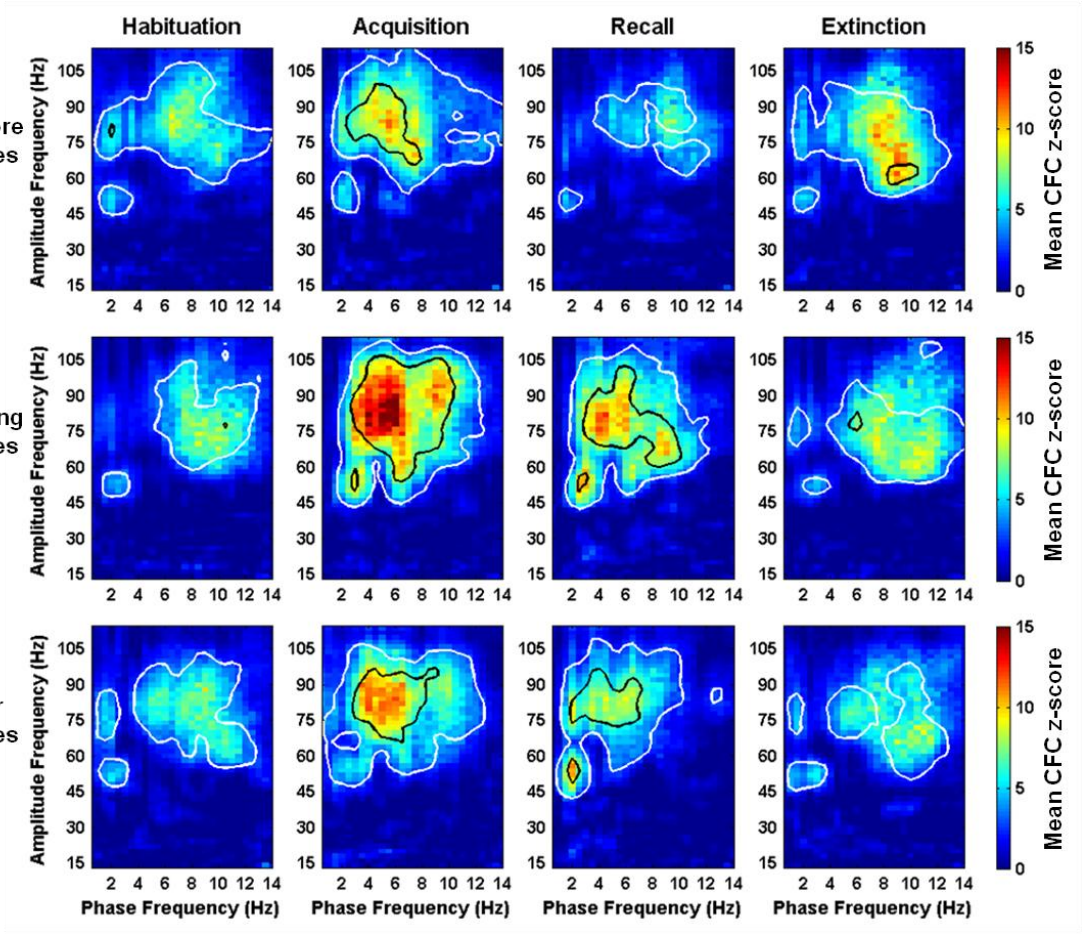
Habituation
Acquisition
Recall
Extinction
A.
Before Tones
B.
During Tones
C.
After Tones
Amplitude Frequency (Hz)
Phase Frequency (Hz)
Mean CFC z-score
105
90
75
60
45
30
15
2 4 6 8 10 12 14
15
10
5
0

Figure 8. Phase preference of significant cross-frequency coupling.

Data expressed in the same format as Figure 6, but representing the mean preferred phase of significant coupling, *i.e.*, the phase bin of the lower frequency band (x-axis) at which the amplitude of the higher frequency band (y-axis) is maximal. Thus, all black pixels represent frequency pairs for which no rats showed significant coupling in that time period and stage of fear learning and extinction. The same significance contours of Figure 6 are copied here for orientation purposes.

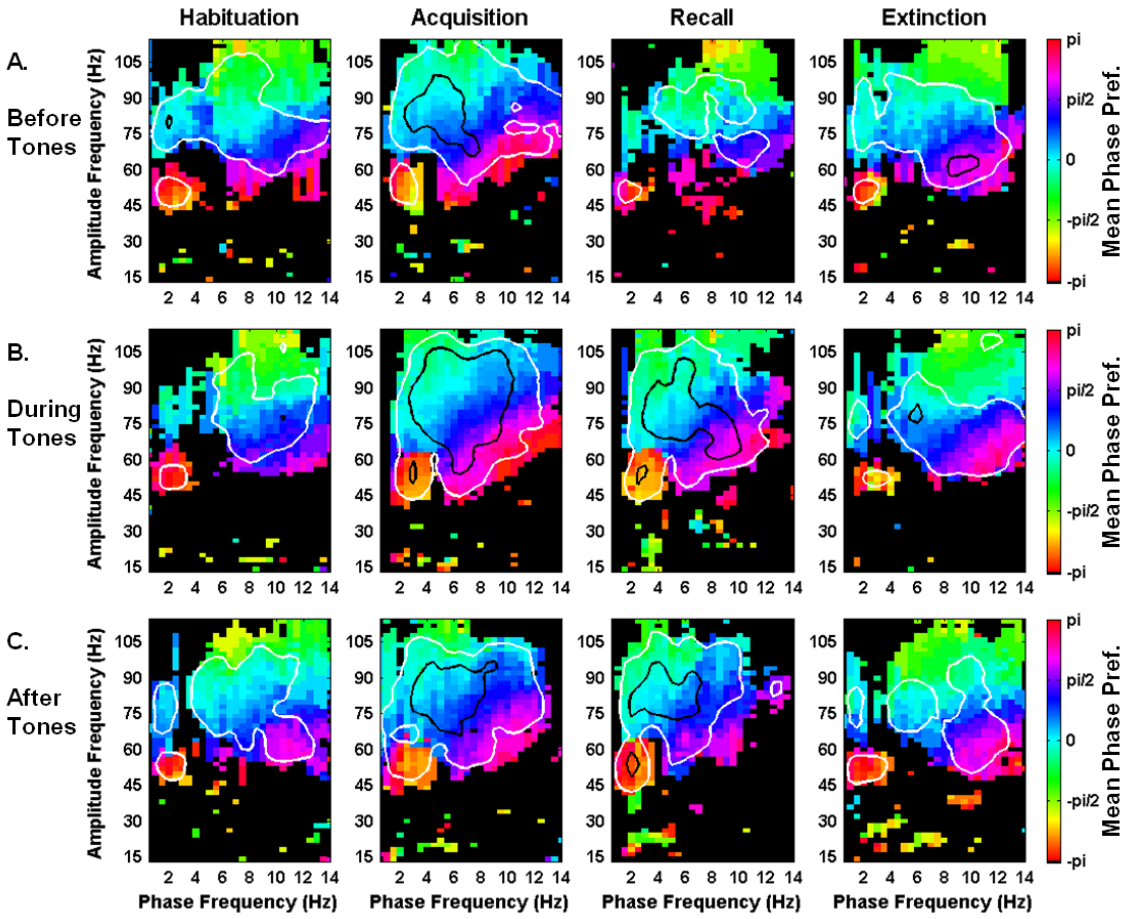
Habituation
Acquisition
Recall
Extinction
A.
Before Tones
B.
During Tones
C.
After Tones
Amplitude Frequency (Hz)
Phase Frequency (Hz)
Mean Phase Pref.
105
90
75
60
45
30
15
2 4 6 8 10 12 14
pi
pi/2
0
-pi/2
-pi